جامعة الإمارات العربية المتحدة
United Arab Emirates University

MASTER THESIS NO. 2022:62

College of Medicine and Health Sciences

Department of Medical Microbiology and Immunology

CORRELATION OF GUT ALTERATION WITH THE PROGRESSION OF EXPERIMENTAL AUTOIMMUNE ENCEPHALOMYELITIS (EAE) IN C57BL/6 MICE

Al Anood Ahmed Ali Aldew Al Naqbi

October 2022

United Arab Emirates University

College of Medicine and Health Sciences

Department of Medical Microbiology and Immunology

CORRELATION OF GUT ALTERATION WITH THE PROGRESSION OF EXPERIMENTAL AUTOIMMUNE ENCEPHALOMYELITIS (EAE) IN C57BL/6 MICE

Al Anood Ahmed Ali Aldew Al Naqbi

This thesis is submitted in partial fulfilment of the requirements for the degree of Master of Medical Sciences (Microbiology and Immunology)

Under the Supervision of Dr. Mariam Al Shamsi

October 2022

Declaration of Original Work

I, Al Anood Ahmed Ali Aldew Al Naqbi, the undersigned, a graduate student at the United Arab Emirates University (UAEU), and the author of this thesis entitled "*Correlations of Gut Alteration with the progression of Experimental Autoimmune encephalomyelitis (EAE) in C57BL/6 Mice"* hereby, solemnly declare that this thesis is my own original research work that has been done and prepared by me under the supervision of Dr. Maryam Al Shamsi, in the College of Medicine and Health Sciences at UAEU. This work has not previously formed the basis for the award of any academic degree, diploma or a similar title at this or any other university. Any materials borrowed from other sources (whether published or unpublished) and relied upon or included in my thesis have been properly cited and acknowledged in accordance with appropriate academic conventions. I further declare that there is no potential conflict of interest with respect to the research, data collection, authorship, presentation and/or publication of this thesis.

Student's Signature:  Date: October 24th, 2022

Advisory Committee

1) Advisor: Maryam Al Shamsi

Title: Associate Professor

Department of Medical Microbiology & Immunology

College of Medicine and Health Sciences

2) Co-advisor: Farah Al-Marzooq

Title: Assistant Professor

Department of Medical Microbiology & Immunology

College of Medicine and Health Sciences

Approval of the Master Thesis

This Master Thesis is approved by the following Examining Committee Members:

1) Advisor (Committee Chair): Dr. Mariam Al Shamsi
   Title: Associate Professor
   Department of Medical Microbiology and Immunology
   College of Medicine and Health Sciences
   Signature _____ Date October 24th, 2022

2) Member: Dr. Zakeya Al Rasbi
   Title: Assistant Professor
   Department of Medical Microbiology and Immunology
   College of Medicine and Health Sciences
   Signature _____ Date October 24th, 2022

3) Member: Saleh Ibrahim (External Examiner)
   Title: Professor
   Director, Division of Genetics
   University of Lübeck, Germany
   Signature _____ Date October 24th, 2022

This Master Thesis is accepted by:

Acting Dean of the College of Medicine and Health Science: Professor Jumaa Al Kaabi

Signature _____ Date 27/October/2022

Dean of the College of Graduate Studies: Professor Ali Al-Marzouqi

Signature _____ Date 27/10/2022

Copy ____ of ____

Abstract

Background: Experimental autoimmune encephalomyelitis (EAE) is the mouse disease model of multiple sclerosis (MS), a chronic autoimmune disease targeting the central nervous system (CNS) resulting in neuroinflammation, neuroaxonal degeneration, and demyelination. Autoreactive $CD4^+$ T cells are known for their role in the pathogenesis of MS. $CD8^+$ T cells and NK cells were also found to be associated with the disease.

Aim: There is a limited number of studies investigating the link between gut alterations and immune cells in the gut influencing the outcome of the disease since the vast majority of MS patients experience gastrointestinal (GI) problems. Here, we correlate alterations in gut microbiota with disease progression along with changes in lymphocytes counts over different time points during the course of the disease.

Method: In the current study, EAE was induced in female C57BL/6 mice with MOG^{35-55} peptide emulsified in the incomplete Freund's adjuvant supplemented with *Mycobacterium Tuberculosis* H37Ra. Flow cytometry was used to assess the level of $CD4^+$, $CD8^+$ T cells, NK cells, and their activation status within the intraepithelial lymphocyte (IELs) throughout the disease progression. This was done along with qPCR analysis to determine the fold change of the selected bacterial species that were previously reported to be altered in MS patients; *Lactobacillus reuteri*, *Prevotella copri*, *Bacteroides fragilis*, *Clostridium perfringens*, and *Akkermansia muciniphila*the. In addition, counts of Paneth cells whose role is essential in maintaining the balance of the normal flora were also investigated by histochemistry.

Results and conclusion: Our results showed no change in the frequencies of both gut $CD4^+$ and $CD8^+$ T cells at all time points, along with an increase in the percentage and activation of gut NK cells at the peak of the disease, a decrease in the beneficial gut normal flora (*Lactobacillus reuteri* & *Prevotella copri*), and significant Paneth cells hyperplasia. Altogether, our results indicate that interactions between gut flora and NK cells may contribute to the pathogenicity of MS.

Keywords: Experimental autoimmune encephalomyelitis, Multiple sclerosis, Gut microbiota, NK cells activity, Cell frequency, Gut/Brain interaction.

Title and Abstract (in Arabic)

العلاقة بين التغيرات المعوية وتفاقم التهاب النخاع الذاتي التجريبي في الفئران (C57BL/6)

الملخص

التهاب النخاع الذاتي التجريبي (EAE) هو نموذج الفأر للتصلب المتعدد (MS)، وهو مرض مناعي ذاتي مزمن يستهدف الجهاز العصبي المركزي (CNS) مما يؤدي إلى التهاب الخلايا العصبية و تدميرها بالإضافة إلى إزالة مادة الميالين (Myelin) التي تحيط بالمحور العصبي و التي تؤدي دوراً مهماً في حماية العصب و نقل الاشارات العصبية . هناك عدة خلايا لها دور كبير في مرض التصلب اللويحي وهي الخلايا التائية ($CD8^+$ T و $CD4^+$ T) والخلايا الطبيعية القاتلة (NK) الغيرمعروف دورها بشكل كامل. الغالبية العظمى من مرضى التصلب العصبي المتعدد يعانون من مشاكل في الجهاز الهضمي (GI).

المثير للدهشة أنه لا توجد الكثير من الدراسات المعنية بالبحث عن الصلة بين التغيرات المعوية والخلايا المناعية الموجودة في الأمعاء والتي تؤثر على شدة المرض. تهدف هذه الدراسة إلى فهم العلاقة بين التغيرات المعوية ونسب الخلايا المناعية في الأمعاء وتأثيرها على المرض. تم تحفيز EAE في إناث الفئران C57BL / 6 بحقنها بالمستحلب المكون من MOG35-55 و incomplete Freund adjuvant و *Mycobacterium Tuberculosis* H37Ra. ثم استخدام تقنية قياس التدفق الخلوي لعد وفحص مستوى الخلايا التائية ($CD8^+$ T و $CD4^+$ T) و الخلايا الطبيعية القاتلة (NK) و نشاطها في الأمعاء الدقيقة (IELs) و ذلك طوال فترة المرض. كذلك تم استخدام تقنية qPCR لتحديد التغيرات في وفرة بعض الفصائل البكتيرية المختارة التي تم رصدها سابقاً عند مرضى التصلب المتعدد و هي كالآتي؛ *Lactobacillus reuteri*، *Prevotella copri*، *Bacteroides fragilis*، *Clostridium perfringens*، *Akkermansia muciniphilathe*. وأيضاً، تم الكشف عن تعداد خلايا Paneth في الأمعاء الدقيقة التي تلعب دوراً أساسياً في الحفاظ على التوازن الطبيعي في الأمعاء وذلك بواسطة تقنية كيمياء الأنسجة (Histochemistry).

نتائج هذه الدراسة تتلخص في زيادة نسبة ونشاط الخلايا القاتلة الطبيعية دوناً عن غيرها من الخلايا في ذروة المرض، وانخفاض في الفلورا المعوية الطبيعية المفيدة وتشمل *Lactobacillus reuteri* و *Prevotella copri*، وتضخم خلايا Paneth. جميع هذه النتائج

تدعم فرضية التفاعل بين فلورا الأمعاء والخلايا الطبيعية القاتلة وأنَّ العلاقة بينهم من الممكن أن تؤثر على شدة المرض والأعراض المصاحبة له.

مفاهيم البحث الرئيسية: التهاب النخاع الذاتي التجريبي، التصلب اللويحي المتعدد، البكتيريا المعوية الطبيعية، تعداد الخلايا، نشاط الخلايا الطبيعية القاتلة.

Acknowledgements

I would like to extend my thanks to Dr. Maryam Al Shamsi who gave me the opportunity to be part of her lab and gave me the chance to start my path in this field. It has been a pleasure to work under her supervision. I am also indebted to Dr. Farah Al Marzooq for her support, wealth of knowledge, and experience she granted me. Her munificent time and her participation in my research have made it possible. Special thanks to Prof. Sherif Karam and his lab members, Dr. Abeer Al Tahrawi, and Prof. Basel Al Ramadi, and his lab team. Also, Dr. Akela for her kindness and help. Many thanks to our medical research specialist Dr. Maya Hassane for standing by me during a tough stage. her assistance towards the difficulties I have faced kept me encouraged and confident.

I am speechless about the symbol of love and giving, my family who have set me off on the road to this journey, and their endless prayers that kept me strong. I'm grateful for my friends Leena Labania and Lana Daoud, I met them at the beginning of this journey and I'm ending it with them, thanks for the continuous support and care. My feelings toward Marah Sawafta are inexplicable, the one who believed in me in the first place and was by my side throughout the hard times. Last but not least, Doua Kamyan, my lab partner and friend, words can't explain how much I'm grateful that I met her, we shared our successes and failures, and we motivated each other the whole time, these 2 years were truly much easier and delighting with her. My gratitude to everyone who offered help and support and to anyone who prayed for me in the unseen and lines missed by mistake.

Dedication

To my beloved parents and family

Table of Contents

List of Tables

List of Figures

List of Abbreviations

APCs	Antigen Presenting Cells
BBB	Blood Brian Barrier
BSA	Bovine Serum Albumin
CFA	Complete Freuend’s Adjuvant
CNS	Central Nervous System
DC	Dendritic Cells
DG Solution	Density Gradient Solution
DTE	Dithioerythritol
EAE	Experimental Autoimmune Encephalomyelitis
ENS	Enteric Nervous System
FACS	Fluorescence Activated Cell Sorting
FBS	Fetal Bovine Serum
GF	Germ Free
GI	Gastrointestinal
H&E	Hematoxylin & Eosin
HEPES	N-2-Hydroxyethylpiperazine-N'-2-Ethanesulfonic Acid
IBD	Inflammatory Bowel Disease
IELs	Intraepithelial Lymphocytes
IFA	Incomplete Freuend’s adjuvant
IL	Interleukin
IP	Intestinal Permeability
i.p	Intraperitoneal
LFB	Luxol Fast Blue
LP	Lamina Propria
LPS	Lipopolysaccharides

MFI	Median Fluorescence Intensity
MHC Class I, II	Major Histocompatibility I, II
MLNs	Mesenteric Lymphatic Nodes
MOG35-55	Myelin Oligodendrocyte Glycoprotein
MS	Multiple Sclerosis
NK Cells	Natural Killer Cells
PAMP	Pathogen Associated Molecular Pattern
PBS	Phosphate Buffered Saline
PPMS	Primary Progressive Multiple Sclerosis
PRMS	Progressive Relapsing Multiple Sclerosis
PTX	Pertussis Toxin
qPCR	Quantitative Polymerase Chain Reaction
RBCs	Red Blood Cells
RPMI	Roswell Park Memorial Institute Medium
RRMS	Relapsing Remitting Multiple Sclerosis
RT	Room Temperature
s. c	Subcutaneous
SPMS	Secondary Progressive Multiple Sclerosis
Th	T Helper Cells
TLR	Toll Like Receptor
UEA I	Ulex Europaeus Agglutinin I

Chapter 1: Introduction

1.1 Introduction to MS

Multiple sclerosis (MS) is a chronic neuroinflammatory autoimmune disease of the central nervous system (CNS). According to Dendrou et al. (2015), around 2.5 million people are diagnosed with MS worldwide, half of them require special care and use wheelchairs by 25 years post-diagnosis. Similar to most autoimmune diseases, females are more susceptible to immune diseases including multiple sclerosis with a female: male ratio of 3:1. So far, there are no early diagnostic tests prior to the appearance of symptoms that vary from one patient to another. A confirmed diagnosis of MS requires initial exclusion of any possible infectious agents causing neurological symptoms by blood tests followed by magnetic resonance imaging (MRI) of the brain and spinal cord for the detection of demyelinated lesions. MS onset usually appears at the age of 30 and the symptoms include muscle stiffness, numbness, fatigue, anxiety, and visual disturbance. In more progressive forms of MS, bladder, bowel, and sexual problems may occur. Patients with severe symptoms may face difficulties in speech and swallowing followed by complete paralysis. The epidemiology of MS is continuously changing and unevenly distributed worldwide; yet, it was shown that the disease is more abundant in the areas away from the equator (Etemadifar et al., 2020; Milo & Kahana, 2010). West Asia including the United Arab Emirates (UAE) recorded the highest prevalence and incidence among Asian countries as revealed in studies conducted between the years 1985-2020. In the UAE, the mean age of the disease onset was about 26 years among Emiratis presenting mostly with visual and motor deficits. Nonetheless, the prevalence rate among the total population was 18/ 100,000 people while it was 57.09/100,000 among native Emiratis and the average annual incidence

rate of MS among Emiratis was 5.4/100,000 between the years 2010 and 2014 (Forouhari et al., 2021).

1.2 Risk Factors of MS

The main cause of the disease is still elusive to this date, but genetic predisposition along with environmental factors are believed to contribute directly or indirectly in developing MS. Genetic predisposition as a factor was confirmed in many studies where family heritability accounts for 20% of MS cases. The specific gene causing the disease is unknown yet, but it was suggested by many studies that HLA allele DRB1*1501 accounts for less than 50% of the total genetic basis of the disease (Milo & Kahana, 2010; Waubant et al., 2019). The risk of developing MS reaches 5.13% among first degree relatives and 25-30% among monozygotic twins. The risk of developing MS even increases by 10 folds in families with both parents diagnosed with the disease (Dyment et al., 1997; Hawkes & Macgregor, 2009). Besides, certain ethnic groups seem to be more resistant to develop MS such as the Mongolian race, Japanese, Chinese, and American Indians which may also be attributed to the genetic predisposition (Ebers, 1992).

Other factors include environmental factors such as UV light, vitamin D deficiency, smoking, diet, and intake of some medications like antibiotics. Recently, gut microbiota is heavily studied as one of the major factors associated with MS. Additionally, a number of infective agents were associated with MS including bacteria and viruses such as *Mycobacterium* and Epstein-Bar virus (EBV), and were employed to induce the disease in animal models (Ascherio & Munger, 2007; Waubant et al., 2019).

1.3 Forms of MS

There are four known forms of MS, the most common presentation is relapsing-remitting (RRMS) form of the disease seen in about 85% of MS patients. RRMS is characterized by courses of an acute neurological condition called relapses and periods of stability between relapses called remission. During relapses, inflammation and demyelination can be visualized by MRI. Remission could vary among patients, some can fully recover, and others recover with lesions in the CNS. The second form of the disease is primary-progressive multiple sclerosis (PPMS), it is seen in approximately 10% of MS patients and is characterized by acute progressive neurological dysfunction since disease onset. The name indicates continuous progression without any remission or defined relapses. The third form of the disease is secondary-progressive multiple sclerosis (SPMS) seen after one or two decades in about 80% of the patients initially diagnosed with RRMS. This form is characterized by initial normal episodes of relapses and remissions until it becomes chronic without remission along with changes in the brain volume and axonal loss. The last and rare form of the disease is the progressive-relapsing multiple sclerosis (PRMS) which affects 5% of the patients and is similar to PPMS except for rare relapses and continuous progression of the disease. Due to its rare presentation, often, PRMS is considered the same form as PPMS. Nevertheless, there is no significant difference in the distribution of the forms of MS worldwide (Dendrou et al., 2015; Lublin et al., 2014).

1.4 Immunopathogenesis

MS is known as T cell-mediated disease yet, initiating factors are not well defined, two hypotheses were suggested as possible scenarios for the disease initiation: the inside-out hypothesis and the outside-in hypothesis (Figure 1).

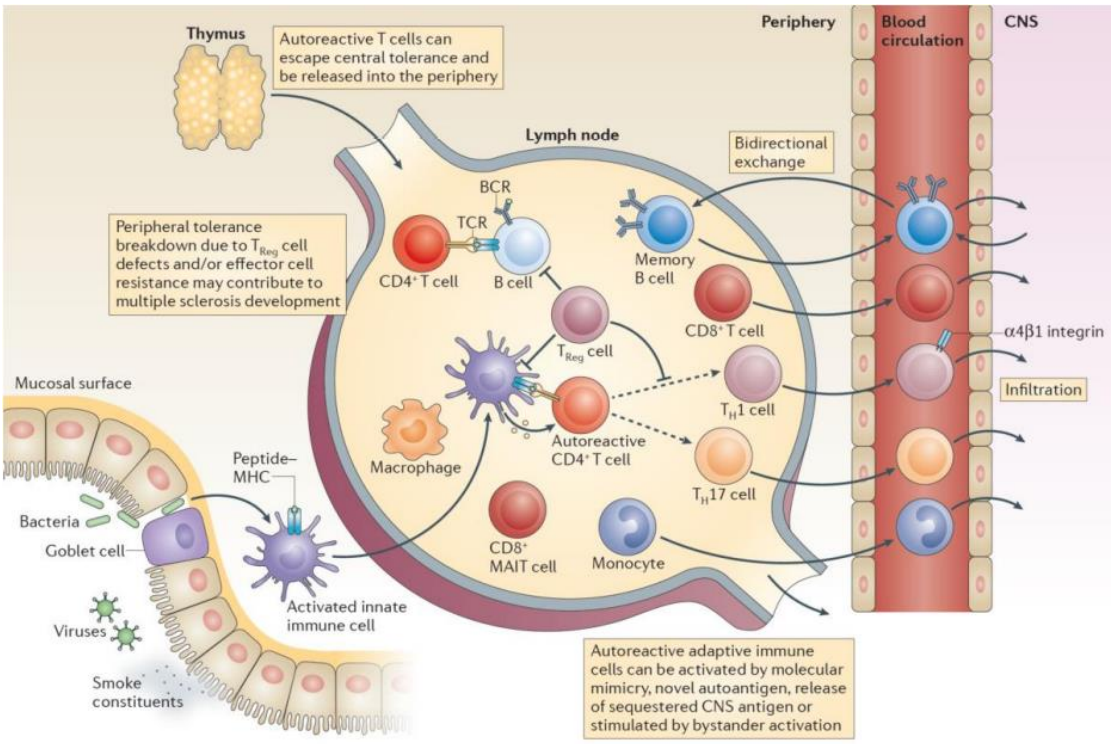

Figure 1: Immunopathogenesis of multiple sclerosis (Dendrou et al., 2015).

The inside-out hypothesis suggests that the damage to myelin sheath starts from the CNS mediated by unknown triggers, most likely these triggers are infectious agents (Pawate & Sriram, 2010). Antigens produced from the destruction of oligodendrocytes are released to the periphery and eventually picked up and processed by antigen-presenting cells (APCs) to induce activation of autoreactive lymphocytes. Activated effector lymphocytes migrate from peripheral lymphatic tissues guided by adhesion

molecules expressed on epithelial surfaces of the blood vessels and chemokines contribute to the breakdown of the blood-brain barrier (BBB) and infiltrate into the CNS. Once there, these T cells are re-activated by CNS resident APCs. Effector autoreactive T cells orchestrate the inflammatory reaction leading to further destruction of the myelin sheath (Titus et al., 2020). The outside-in hypothesis is explained by molecular mimicry where the initiation of the process is in the periphery rather than in the CNS. The trigger here is suggested to be an infectious agent such as viruses with structural similarities to the myelin protein which is taken up by peripheral APCs that trigger the activation of autoreactive T cells (Dhaiban et al., 2021). Generally, T cells differentiate upon activation to their subsets and release cytokines that recruit other immune cells like T, B, and NK cells from the periphery to the CNS. Such cytokines disrupt the BBB which allows the recruited cells to pass through it contributing to the elimination of the cognate myelin antigen (Dendrou et al., 2015; Dhaiban et al., 2021). Further, Dhaiban et al. (2017) suggested that the disruption of BBB may be mediated through the adhesion of integrins found on $CD4^+$ T cells to the BBB, facilitating their migration; such integrins are lymphocyte function associated antigen (LFA-1) and the very late antigen-4 (VLA-4). In normal conditions, self-tolerance to self-antigens is achieved by either deletion of autoreactive T lymphocytes in the thymus (Central tolerance) or suppressing their activation in the periphery (Peripheral tolerance). Factors involved in the activation of autoreactive T cells include the expression of co-stimulatory molecules on APCs and the activity of immunosuppressive T regulatory cells (T_{reg}) (Danikowski et al., 2017; Dendrou et al., 2015).

Most likely, tissue damage occurs when activated T cells migrate to the CNS and get reactivated in response to myelin antigens presented on APCs, but more studies

reported that tissue damage is also linked to the overproduction of glutamate, an excitatory neurotransmitter, reactive oxygen species (ROS) and reactive nitrogen species (RNS) within the CNS. Activated glial cells produce glutamate and cause an elevation in its levels in MS lesions whereas its overproduction leads to the overexcitement of the nerve cells and their damage (Pitt et al., 2000). Additionally, the production of reactive oxygen species (ROS) and reactive nitrogen species (RNS) by the activated macrophages and microglia in the CNS cause mitochondrial dysfunction and reduces the supply of energy to the neurons leading to axonal damage (Fischer et al., 2012; McMahon et al., 2005).

Besides, effector $CD4^+$ T cells, B cells, monocytes/macrophages, $CD8^+$ T cells, and NK cells are the cells that migrate from the periphery to the CNS after disrupting the BBB (Dendrou et al., 2015; Dhaiban et al., 2021). The role of $CD4^+$ T cells, $CD8^+$ T cells, and NK cells is discussed in details through this study.

1.4.1 $CD4^+$ T Cells

$CD4^+$ T adaptive lymphocytes play an essential role in orchestrating immune responses following activation by their specific antigen through engaging and activating other immune cells like B cells and subsets of T cells. Additionally, it is believed that $CD4^+$ T cells are among the main contributors to the development of MS. Therefore, the presence of activated $CD4^+$ T cells in MS lesions, blood, and in the cerebrospinal fluid (CSF) of MS patients is expected compared to normal individuals (J. Zhang et al., 1994). Two main subsets of $CD4^+$ T cells were linked with the pathogenesis of MS; T helper 1 (Th1) and T helper 17 (Th17). Activation of naïve $CD4^+$ T cells requires recognition of its specific antigen presented on the MHC class II on the surface of APCs, along with engaging co-stimulatory molecules. Activated

$CD4^+$ T cells then differentiate into effector and memory cells of different T cells subsets influenced by the cytokines released. Differentiation into different $CD4^+$ T cells subtypes is also regulated by the binding affinity of T cell receptor and MHC/antigen complex; when MHC class II antigen is expressed in high density, $CD4^+$ T cells differentiate to either Th1 or Th17, unlike the case with low affinity binding leading to the differentiation into Th2 (Luckheeram et al., 2012). Different subsets of activated $CD4^+$ T cells have different cytokines signature, Th1 cells secrete IFN-γ, interleukin (IL) 2, and TNF while Th17 cells secrete IL-17 or IL-22, and Th2 cells secrete IL-4, IL-5, IL-10, and transforming growth factor (TGF)-β (Chitnis, 2007; Delgado & Sheremata, 2006; Dhaiban et al., 2021). According to Chitnis (2007), high levels of Th1 cytokines were detected in the brain tissue and CSF of MS patients. Moreover, adoptive induction of the disease in mice models by transferring myelin specific Th17 cells to normal mice resulted in a more severe form of the disease (Langrish et al., 2005). Essential contribution of IFN-γ was also concluded following studies on experimental autoimmune encephalomyelitis (EAE) where the diseases was exacerbated in the group treated with IFN-γ at the initial stage of the disease (Naves et al., 2013).

1.4.2 $CD8^+$ T Cells

$CD8^+$ T adaptive lymphocytes are, cytotoxic and, were suggested to be active players in MS as evident by their high frequency in the brain lesions of MS patients. $CD8^+$ T cells also require prior activation by APCs for their recruitment to the CNS. Migration of $CD8^+$ T cells into the CNS and through the BBB is facilitated by chemokines and the expression of adhesion molecules on the surfaces of the CNS endothelial cells such as P-selectin (Dhaiban et al., 2021; Traugott et al., 1983). CNS antigen-specific $CD8^+$

T cells are involved in CNS damage during relapses and in the chronic phases of MS. Damage is mediated by $CD8^+$ T cells involve inducing apoptosis of oligodendrocytes expressing self-antigens presented on MHC I molecules, this process is mediated by the release of perforin, granzyme A (GzmA) and granzyme B (GzmB) into the target cells (Barry & Bleackley, 2002). Additionally, the adoptive transfer of $CD8^+$ Myelin oligodendrocyte glycoprotein (MOG) specific T cells, resulted in more severe, and long-lasting relapses. Furthermore, $CD8^+$ T cells are believed to contribute to the pathogenesis of MS through the secretion of their cytokines like IFN-γ and IL-17 (Huber et al., 2012).

1.4.3 NK Cells

Natural killer (NK) cells are large granular lymphocytes of the innate immune system and are known for their effective role in selectively targeting tumor cells and virally infected cells for destruction without prior sensitization. Beyond that role, NK cells were appreciated for their impact on the modulation of adaptive immune responses in inflammatory and autoimmune responses through their cytolytic activity, cytokines secretion, and dendritic cells (DC) editing (Caligiuri, 2008). Dendritic cells editing is when NK cells target dendritic cells not expressing MHC class I (Immature cells) for destruction and spare mature dendritic cells which migrate to the lymphoid organs promoting T cells priming (Ferlazzo & Moretta, 2014).

Human NK cells subsets are identified by their differential expression of CD16 and CD56 on their surfaces. $CD16^-$ $CD56^{bright}$, also known as immature NK cells, make less than 10% of total blood NK cells, while they are more abundant in tissues and are able to produce large amounts of cytokines upon stimulation. On the other hand, $CD16^+$ $CD56^{dim}$ or mature NK cells represent around 90% of total peripheral blood

NK cells, while they are less abundant in tissues, but are efficient killer cells and are able to secrete high levels of IFN-γ. Murine NK cells do not express CD56 yet, they express CD27; $CD3^{-}$ $CD27^{high}$ are equivalent to $CD16^{-}CD56^{bright}$ whereas $CD3^{-}$ $CD27^{low}$ are the murine equivalent to human $CD16^{+}CD56^{dim}$. Even though cytotoxicity was mainly attributed to the effect of $CD16^{+}$ $CD56^{dim}$, $CD56^{bright}$ NK cells can lyse activated T cells through a granzyme K mediated mechanism (Caligiuri, 2008). Degranulation of these cells causes caspase independent apoptosis and mitochondrial dysfunction in activated T cells by preferential transfer of granzyme K (Jiang et al., 2011). Furthermore, NK cells express various receptors including activating, costimulatory, and inhibitory receptors to enhance their role through their interaction with their ligands. The two major receptors expressed on NK cells are activation (NKG2D) and inhibitory (NKG2A) receptors that contribute to the regulation of cytokines production and cytotoxic killing capacities of NK cells. Under normal conditions, inhibitory signals dominate which keeps NK cells inactive. In cases where NK cells activation receptors recognize stress markers on target cells activation signals prevail causing loss of equilibrium and activation of NK cells (Dhaiban et al., 2021; Winkler-Pickett et al., 2008).

NKG2D is expressed at the very early stages of NK cell precursor starting relatively low but its expression increases and remains high as NK cells go through their maturation stages (Abel et al., 2018). NKG2D represents a major recognition receptor for the detection of damaged, transformed, and pathogen-infected cells. However, persistent exposure to cells expressing NKG2D ligand results in the decrease of NKG2D surface expression. This, in turn, results in functional impairment of NKG2D dependent NK cell functions (Molfetta et al., 2017). Moreover, NKG2D contribute in

the disruption of oligodendrocytes so, blocking the interaction between NKG2D and its ligand diminished the disruption of these cells mediated by the activated receptor (Saikali et al., 2007).

Killer cell immunoglobulin-like receptors KIRs and NKG2A are inhibitory receptors on NK cells that allow NK cells to distinguish self-cells from non-self cells. This is achieved mainly by surveying the expression of MHC-I molecules on target cells. Expression of MHC-I molecules on target cells engages NK cell inhibitory receptors and protects targeted cells from the destructive action of NK cells. Therefore, lack of MHC-I expression leads to NK cells activation (X. Zhang et al., 2019). HLA-E in human (Qa-1 in mice) was found to be increased in the white matter of MS patients compared to healthy individuals which may explain the impaired function of NK cells in MS patients. Detection of HLA-E/Qa-1 expression on autoreactive cells by the NK cells inhibitory receptor suppresses the killing of the autoreactive cells mediated by NK cells. Hence, the severity of the disease was reduced when the interaction between NKG2A and its ligand was blocked (Durrenberger et al., 2012; Gulla & Thompson, 2021; Lee et al., 1998). Studies by Sun et al. (2016) on patients with liver cancer concluded that NK cells with higher NKG2A expression exhibited characteristics of functional exhaustion, such as lower IFN-γ production and weaker cellular cytotoxicity, as well as a shorter overall survival.

The role of NK cells in MS or EAE was intensively studied, but yielded contradictions on whether they contribute to the pathogenesis or play a regulatory role. Studies supporting the regulatory role of NK cells suggested that NK cells during the course of EAE in C57BL/6 mice showed reduced functional activity during relapses compared to times of remissions during which, NK cells activity increased. There are

3 reported ways by which NK cells regulate the disease, suggested through either direct killing of autoreactive T cells, through supporting astrocytes to kill autoreactive T cells (Sanmarco et al., 2021), or by inhibiting the proliferation of autoreactive T cells (Yokoyama, 1998; B. Zhang et al., 1997). Furthermore, in support of the regulatory role of NK cells on the disease progression, depletion of NK cells prior to disease induction in SJL/J mice yielded more severe symptoms compared to the control group (Xu et al., 2005; Xu & Tabira, 2011). On the other hand, the pathogenic role of NK cells was proved in EAE by depleting NK cells at early stages where the clinical scores were lower in depleted diseased mice compared to control (Dungan et al., 2014; Winkler-Pickett et al., 2008). Dungan et al. (2014) suggested that NK cells contribute to the pathogenesis of MS by producing IFN-γ polarizing macrophages to M1 phenotype that produce proinflammatory cytokines. From another point of view, the contact between NK cells and neural stem cells (NSCs) induces the release of IL 15, which is essential for NK cells proliferation. At the same time, NK cells also induce the killing of the neural stem cells (NSCs) since they do not express Qa-1, thus contributing to CNS damage (M. Liu et al., 2021; Q. Liu et al., 2016)

1.5 Animal Models of the Disease

EAE is an animal model of MS that was discovered accidentally in the late 19th century. This model was used on rodents, rabbits, and monkeys to understand the pathogenesis and the factors contributing to MS. EAE can be actively induced by the administration of an antigen emulsified in an adjuvant and supported with a toxin to create an autoimmune response cognate to MS. The form and severity of the induced disease varies depending on the species used, strain, type of administered antigen, its route of administration, and its dose. In addition, EAE can also be induced passively

by transferring the activated autoreactive T cells from diseased to healthy animals (Ruppova, 2017).

1.5.1 Active EAE

C57BL/6 mice now are widely used for EAE model as their genes can be easily modified compared to other mice strains. Different mice strains and antigens were used depending on the aim of the study. Previously, SJL/J mice were used when the study focused on the relapsing-remitting form of EAE while C57BL/6 were used to study the progressive form of the disease. Later on, the C57BL/6 strain was used regardless of the disease form through manipulating the given doses of the same antigen, myelin oligodendrocyte glycoprotein (MOG). Administration of a low dose of MOG35-55 in C57BL/6 mice resulted in a relapsing-remitting form of the disease whereas when the dose increased, a chronic form was observed. Other autoantigens used to induce the disease are: myelin basic protein (MBP) and proteolipid protein (PLP) (Rangachari & Kuchroo, 2013; Ruppova, 2017). It is important to note that all antigens were administered as an emulsion composed of the antigen emulsified in Freund complete adjuvant (FCA) or incomplete Freund adjuvant (IFA) supplemented with *Mycobacterium tuberculosis*. The use of the adjuvant is to enhance the immunogenicity of the introduced autoantigen and the mycobacterium is for the stimulation of toll like receptors (TLRs) to enhance the production of the proinflammatory cytokines. The emulsion has to be administered subcutaneously, through the flanks, base of the tail, or between shoulder blades. Pertussis toxin is administered intraperitoneally along with the emulsion in order to support the disruption of the BBB and invasion of the CNS by autoreactive T cells and other

immune cells (Bert et al., 2011; Constantinescu & Hilliard, 2005; Namer et al., 1994; Peiris et al., 2007).

1.5.2 Passive EAE

Passive induction of EAE is achieved by the adoptive transfer of myelin-specific T cells. In this model, EAE is induced in a group of mice as previously described and this is followed by isolation of autoreactive T cells. Autoreactive T cells are then administered intraperitoneally into a normal mouse. One of the advantages of the passive over the active induction of EAE is to avoid infections that might result from injecting CFA or the emulsion itself (Naparstek et al., 1983; Ruppova, 2017).

1.6 Microbiota

Microbiota defines a collection of all kinds of microbes within a certain habitat and it varies between individuals or even within different parts of the same host (Shahi et al., 2017). Trillion microbes including viruses, bacteria, archaea, and eukaryotes inhabit the human body. Around 10^{14} of these microbes are found in the gastrointestinal (GI) tract, while 10^{12} microbes represent the skin microbiota, and the rest colonize other body parts such as hair, urinary, and respiratory tracts. Alteration in the composition of the normal flora is termed dysbiosis. Moreover, due to the large count and diversity of the microbiota, it is believed to contribute significantly to the general status of the host in health or disease through their interactions with the immune system (Jandhyala et al., 2015; Thursby & Juge, 2017). It is well established through studies on germ-free mice that colonization of the mammalian host's mucosal surfaces with microbiota in early-life plays a critical role in the maturation of the host immune system. Chung et al. (2012), revealed that the gut intraepithelial lymphocytes (IELs) were lower in

count, and the size of Peyer's patches and mesenteric lymph nodes (MLNs) were reduced in germ free (GF) mice compared to colonized mice. Composition and diversity of the microbiota are thought to be acquired at birth and are also influenced by many factors including mode of delivery at birth, diet, medications, environment, exposure to pathogens, age, gender, and other factors (Heiss & Olofsson, 2019). Several studies showed that cesarean delivery and formula-feeding are associated with high incidences of infection and allergy diseases (Azad et al., 2013; Madan et al., 2016).

1.6.1 Interaction between Gut Microbiota and Immune Cells in the Gut

Human gut composes of 5 x 10^{10} lymphocytes, five folds the number of lymphocytes found in the blood (Blum & Pabst, 2007). These lymphocytes are distributed in different regions of the intestine; MLNs, lymphoid follicles, lamina propria, Peyer's patches, and between epithelial cells which they are intraepithelial lymphocytes (IELs). In humans, the majority of immune cells in the gut are $CD4^+$ T cells which are normally more abundant in the lamina propria while $CD8^+$ T cells are more abundant within the IELs. As for NK cells, they are found scattered in the lamina propria and along the epithelium; between the epithelial cells in particular (Goodier, 2010). The same distribution was found in C57BL/6 mice where, 90% of IELs were $CD8^+$ T cells and the NK cells ($CD3^-$ NK 1.1^+) around 0.7% and 2% of total IELs (López & Holmes, 2005; Martin et al., 2001). All gut immune cells including dendritic Cells (DC), NK cells, $CD4^+$, and $CD8^+$ T cells interact with each other to maintain the gut homeostasis through continuously sampling the microenvironment and effectively interacting with both pathogenic and non-pathogenic bacteria. Briefly, NK cells interact with gut microbiota through their expressed TLR2, TLR3, and TLR9 and their

activation results in the secretion of the cytokines IFN-γ, TNF, IL-2, IL-17, and IL-22 which activate macrophages to induce phagocytosis. Later, an adaptive immune response initiates and these cytokines subsequently influence the differentiation of T cells contributing to the elimination of pathogenic bacteria (Aziz & Bonavida, 2016; Poggi et al., 2019; Satoh-Takayama et al., 2008).

Studies on the interaction between the gut commensals and immune cells revealed that the activation of immune cells is directly or indirectly modulated by the gut flora in several possible ways (Figure 2). In general, enteric bacteria produce ligands that are recognized by DC via Pattern Recognition Receptors (PRRs) inducing the release of their cytokines including IL-12 that promote the secretion of GzmB by NK cells inducing apoptosis of the stressed cells, and the secretion of IFN-γ which facilitate the differentiation of Th1 (Castleman et al., 2020; Espinoza & Minami, 2018; Fink et al., 2007; Rizzello et al., 2011). Furthermore, administration of polysaccharide A derived from *Bacteroides fragilis* to GF mice inhibits Th17 development and induces T_{reg} cells' accumulation by engaging with TLR-2 expressed by T cells. On the other hand, segmented filamentous bacteria (SFB) were proved to induce a Th17 immune response while *Clostridium* promotes T_{reg} cell induction. Also, Geva-Zatorsky et al. (2017) found that gut Th17 cells expanded as a result of the increase in the abundance of *Acinetobacter baumannii* and *Porphyromonas uenonis* as well as segmented filamentous bacterium (Candidatus Arthromitus).

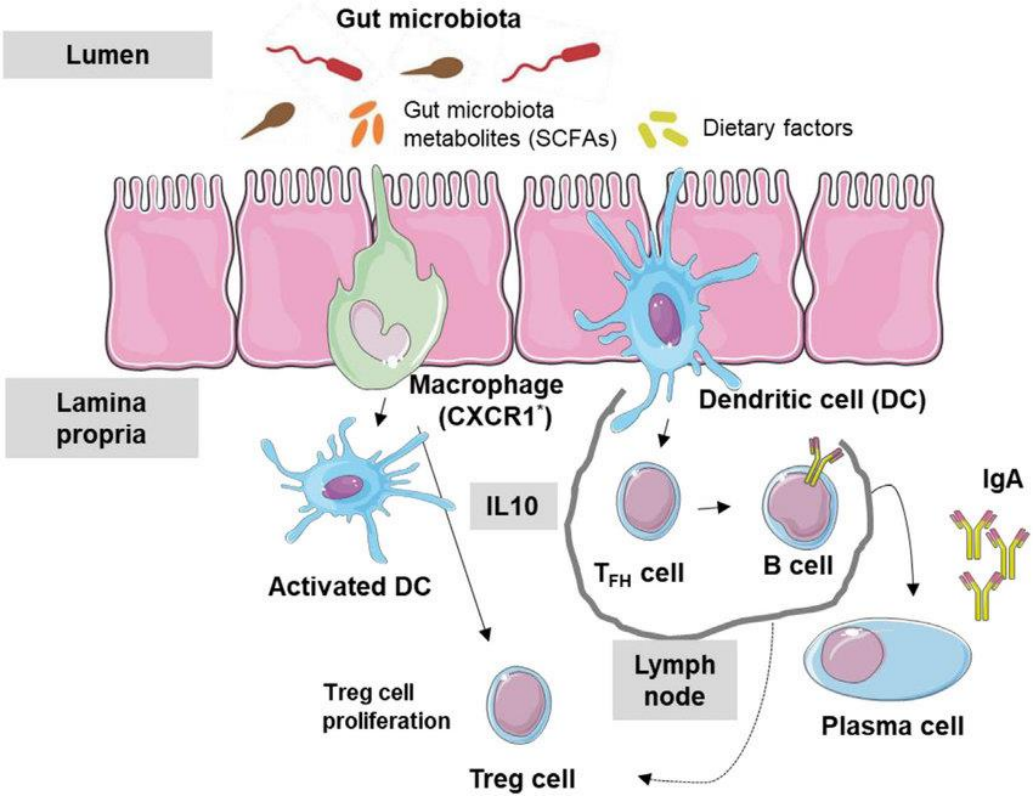

Figure 2: The influence of gut microbiota on the immune cells in the gut (Pascal et al., 2018).

Ganal et al. (2012) support the interaction between gut microbiota and NK cells; GF mice showed impaired NK cell response compared to the specific-pathogen-free. It is suggested that IFN-γ genes required an instructive signal from gut microbiota which was impaired in the GF mice. Consequently, the IFN-γ response in germ-free mice was impaired compared to specific-pathogen-free, leading to reduced priming of cytotoxic lymphocytes. In addition, Aziz & Bonavida (2016) reported that administration of *Bifidimona lactus* as a probiotic for 3 weeks to healthy individuals increased both the number of NK cells and their activity. Moreover, a study showed that dysbiosis in patients with inflammatory bowel disease leads to the activation of the DNA damage response (DDR) that leads to the expression of NKG2D ligands on

the stressed cells, which activates NK cells to eliminate them (Espinoza & Minami, 2018).

1.6.2 Gut/Brain Axis

The GI tract is characterized by its own set of neurons which interact with the CNS to maintain the GI functions, such system is called enteric nervous system (ENS). ENS is responsible of keeping the intestinal barrier intact, controlling the regulation of fluids exchange, controlling epithelial and the function of Paneth cells that secrete antimicrobial peptides to maintain the gut microbiota. Paneth cells also play an important role in controlling the intestine motility, and digestion (Braniste et al., 2014).

1.6.2.1 Microbiota and Immune cells in the CNS

Gut microbes were found to be associated with the immune cells in the gut as well as the immune cells in the CNS. Haghikia et al. (2015), proposed that gut microbiota components trigger the expansion or suppression of the proliferation of gut immune cells that eventually influence the immune cells in the CNS. In EAE model, SCFAs expanded T_{reg} cells and ameliorate the disease whereas long-chain fatty acids promote the expansion of Th1 and Th17 cells worsening the disease (Figure 3A).

The role of gut microbiota in supporting the maturation and function of immune cells is not restricted to immune cells in the periphery, but also to resident immune cells in the tissues such as in the CNS. Microglia are the specialized CNS resident innate immune cells that maintain CNS health by responding to any local infection or tissue damage like the case of MS (Thompson & Tsirka, 2017). Several studies demonstrated that gut microbes influence the maturation and the function of microglial cells. For instance, GF mice showed a change in the microglial cells morphology and a higher

number of immature microglial cells in the brain (Erny et al., 2015). Meng et al. (2015) suggested that SCFAs produced by certain microbes are important for the microglial cells maturation through their binding to GPR43 expressed on microglial cells (Figure 3B) (Erny et al., 2015). Introducing SCFAs to GF mice postnatally compensated the maturation status of the microglia cells in the brain to a level similar to the normal mice (Erny et al., 2015).

1.6.2.2 BBB

The blood-brain barrier is known for its selective permeability and its function to maintain tight regulation of the movement of ions, molecules, immune cells, and infective agents between the brain and blood though restricting the access to substances with low molecular weight, and a high lipid soluble properties (Banks, 2009). Gut microbes produce components with such characteristics as SCFAs that can pass through the membrane easily and interact with immune cells including microglia thus, they are believed to have a role in modulating the BBB permeability. According to Banks (2009) and Braniste et al. (2014), the BBB was disrupted in GF mice and the expression of tight junction proteins (Occludin and claudin-5) was reduced (Figure 3C). Administration of SCFAs restores the permeability of the BBB to its normal status as well as the colonization with *Clostridium tyrobutyricum* that secretes butyrate, which has the capacity to cross the BBB.

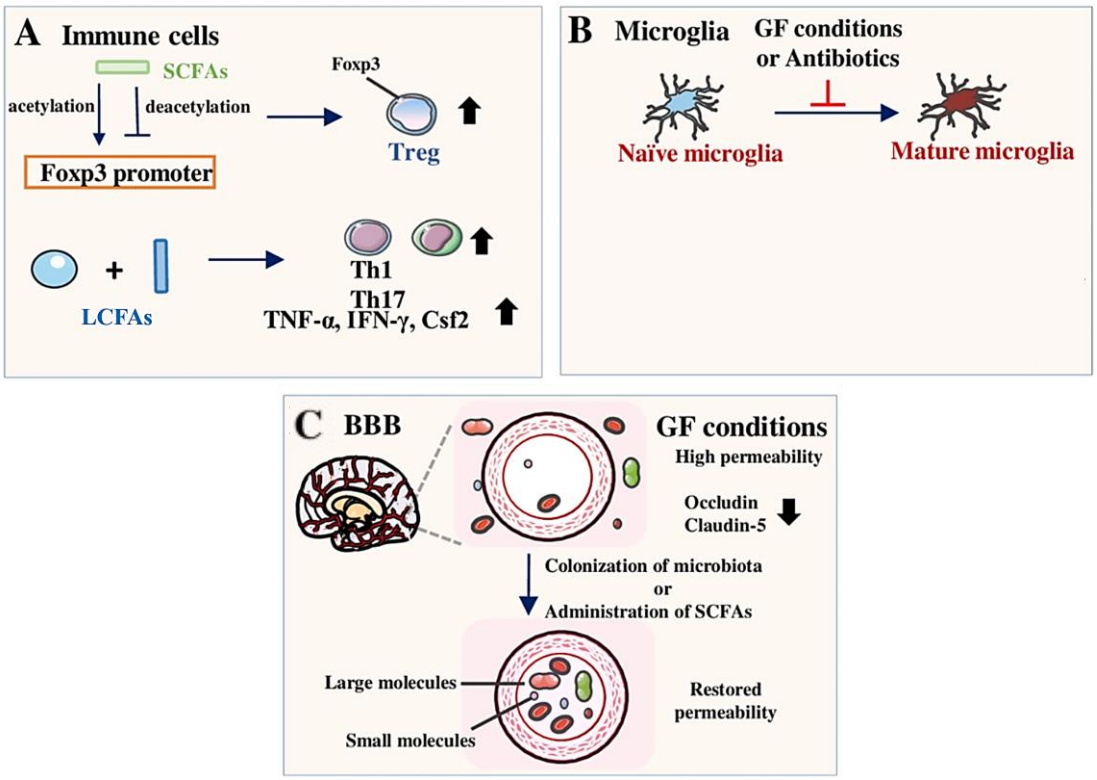

Figure 3: Influence of the gut microbiota on different components in the CNS (et al., 2019).

1.6.3 Role of Microbiota in MS

Gut commensals interact with the mucosal immune cells and maintain CNS physiology at the same time; thus, it is believed that they play a vital role in the initiation or progression and severity of MS. A possible scenario explaining the disruption of the BBB, peripheral autoreactive $CD4^+$ T cells are activated and secrete proinflammatory cytokines in response to the changes in the gut microbiota, these cytokines contribute the disruption of BBB mediating the migration of the immune cells to the CNS to initiate the disease. Also, low graded endotoxemia was detected among MS patients due to the increased levels of the endotoxin lipopolysaccharide (LPS) released by killed bacteria, is thought to be the result of dysbiosis and subsequent change in the intestinal permeability (IP) and BBB. LPS and LPS protein

are known to exert proinflammatory actions on microglia and astrocytes and are therefore believed to be the main contributors to the BBB perturbation (Buscarinu et al., 2019). Another theory suggests that stimulation by microbiota components or diet results in high levels of zonulin, a protein synthesized in intestinal and liver cells that reversibly regulates intestinal and BBB permeability through modulating the gut junctions. A recent study showed that exposure to Gram-negative bacteria regardless of their virulence increases the secretion of zonulin that was found high in MS patients during relapses. Zonulin levels returned to normal during remissions (Fasano, 2020; Jian et al., 2022).

Further confirmation on the role of modulations of gut microbiota in the maturation of the immune responses and the pathogenesis of the disease is provided through studies on GF mice which were found to have a certain degree of resistance to develop EAE compared to normal mice (Berer et al., 2011). Same results were obtained with Stanisavljević (2018) between the two groups, but treating a third group of naïve mice with antibiotics before the induction cause the disease to develop normally (Stanisavljević et al., 2018). In addition, transplantation of identified pathogenic bacteria from MS patients into GF mice resulted in exacerbation of induced EAE with detected expansion in Th1 and Th17 subsets and down regulation of T_{reg} cells (Boussamet et al., 2022; Schroeter et al., 2021). According to Wells et al. (2017), gut commensals maintain IP intact through the production of short-chain fatty acids (SCFA) that maintain the tight junctions and the activation of TLR on NK cells. In contrast, modifications of the gut microbiota contribute to the disruption of the gut barrier and to EAE. Findings of Nouri et al. (2014), demonstrated overexpression of the tight junction protein zonulin in LP and IELs, a significant increase in the zonulin markers in the plasma of the blood, this was detected at score 1 and increased

significantly at score 2 compared to the control group where the levels remained stable. In addition, progression through the clinical scores of the disease was also found to be associated with the overall change in the morphology of the intestine, mainly the enlargement of the microvilli and epithelial cells (Nouri et al., 2014). Nevertheless, Johanson et al. (2020) investigated the microbial composition at different stages of the disease; pre-immunization, post-immunization, disease onset, and finally, at the peak of the disease, they found that the microbiota started to change few days post-immunization.

MS patients are inhabited by specific bacteria that are not abundant in healthy individuals and most of these patients suffer from gastrointestinal problems following their MS diagnosis (Ochoa-Repáraz, Magori1, et al., 2017). Gut microbiota induces either proinflammatory or anti-inflammatory response depending on the specie, whether it is pathogenic or not (Gödel et al., 2020). Most studies focused on the genomic sequencing of bacterial families from stool samples and abundancy or decrease in certain families were correlated to disease severity in MS and EAE. Up till now a number of bacterial families were found to be strongly associated with MS, but the same was not confirmed for all of these microbial groups in animal models of the disease. In the present study, the following bacterial species were investigated.

Lactobacillus reuteri:

Lactobacillus reuteri is a Gram-positive, rod-shaped bacteria colonize the gut of most mammals. In EAE, the family was found dominant in the gut of all mice before immunization, but it decreased post-immunization in diseased mice while remained almost the same in naïve group. *Lactobacillus ruteri* is suggested to have an anti-inflammatory role in autoimmune diseases and is currently utilized as a probiotic that

was found to be effective in minimizing the severity of MS (Chen et al., 2016); Freedman et al., 2018; Gandy et al., 2019; Johanson et al., 2020; Shahi et al., 2017).

Prevotella Copri:

Prevotella copri is a Gram-negative anaerobic bacterium, non-spore forming. It is the most common bacteria of the *Prevotella* genus that occupy the human gut, with estimates indicating ~ 40% prevalence among all *Prevotella* species (Tett et al., 2019). *P. copri* is often linked with desirable health measures including improved glucose metabolism, and reduced visceral fat, yet conflicting reports also exist linking this specie to insulin resistance, hypertension, and persistent gut inflammation. In MS, frequency of *P. copri* was reported to be reduced in RRMS patients, but increased in treated patients suggesting a negative correlation of this specie with the disease in human, but not much was reported in EAE (Freedman et al., 2018; Shahi et al, 2017). Bacteria from this genus proposed to have a role in the protection against the disease (Baecher-Allan et al., 2018).

Akkermansia muciniphila:

Akkermansia is a Gram-negative oval shaped mucin-degrading bacterium. This genus increased among MS patients. In mice, the species *Akkermansia muciniphila* is absent in normal SJL/J mice, while found in normal C57BL/6 mice. Another study showed that this species is found to be more associated with the chronic progressive form of EAE than RRMS (Baecher-Allan et al., 2018; Freedman et al., 2018; Gandy et al., 2019; Shahi et al., 2017). Moreover, *In vitro* study revealed that *A. muciniphila* promotes the differentiation of Th1 cells.*Clostridium perfringens*

Clostridium perfringens is an anaerobic Gram-positive spore-forming bacillus that is associated with acute gastrointestinal infections. *Clostridia* families including *Clostridiaceae,* and *Ruminococcaceae* were abundant in mice following disease induction. However, contradictory results were found for *Clostridium*, as Cantarel et al. (2015) and Miyake et al. (2015) reported a reduction in the abundance of *Clostridium* in MS. The enrichment of this species in samples of MS patients was mainly attributed to their association with supporting the differentiation of the proinflammatory Th17 cells and the role of their produced toxins in compromising the BBB (Lee YK., et al., 2011; Johanson et al., 2020).

Bacteroides fragilis:

Bacteroides fragilis, is an obligate anaerobic Gram-negative bacillus and is part of the normal microbiota of the human colon. *B. fragilis* was detected in low levels in MS patients compared to control and its capsular polysaccharide is believed to have an immunomodulatory effect through inducing the secretion of the anti-inflammatory cytokine IL-10 from regulatory T cells (Gandy et al., 2019; Johanson et al., 2020).

1.7 Paneth Cells

The small intestine is divided into the duodenum, jejunum, and ileum; each is surrounded by lumen which contains cells having microvilli, and between the microvilli there are intestinal glands called crypts. Paneth cells are found at the bottom of the crypts of Lieberkühn in the small intestine mostly. These cells secrete mucus and antimicrobial peptides like Reg3 lectins (Reg3A in humans and its ortholog Reg3γ in mice), lysozyme, secretory phospholipase A2 isotype II (PLA2G2A), and α-defensin peptides to prevent pathogen invasion. These peptides also maintain and

support healthy composition of gut flora through their contribution to the elimination of pathogenic bacteria via their interaction with surface peptidoglycan of Gram-positive bacteria as an example. Therefore, it is not surprising that manipulation of the Paneth cells function or their secreted peptides can lead to dysbiosis (Chairatana & Nolan, 2017; Lueschow & McElroy, 2020; Salzman & Bevins, 2013). The cell count and activity of Paneth cells were found to be altered in response to stress as a result of infection. In the case of HIV patients, the counts of Paneth cells were reduced, and their functions were greatly compromised. On the other hand, Paneth cells counts were increased in IBD patients (Kelly et al., 2004). It is therefore believed that providing probiotic supplementation can help in restoring the counts and functions of Paneth cells (Cazorla et al., 2018).

1.8 Aims and Objectives

It is well known that MS is associated with changes in the gut microbiota, but it is not defined yet whether MS changes the composition of the gut immune cells and microbiota or vice versa. Additionally, many studies were designed to understand the role of NK cells and other lymphocytes in the immunopathogenesis of the disease neglecting the correlation of these cells with the changes in the gut microbiota and how this interaction influences the severity of the disease.

This study aims to correlate modifications in the level of selected bacterial strains as a result of EAE induction with disease progression and immune cells frequency in C57BL/6 mice. This will be achieved by:

1. Investigating levels of circulating and intestinal $CD4^+$, $CD8^+$ T cells, and NK cells utilizing the MOG induced model of EAE in C57BL/6 mice at 3 different

time points, prior to disease induction, at disease onset, and later at the peak of the disease.

2. Investigating the levels of activation and inhibitory receptors expression on the surfaces of circulatory and intestinal NK cells at the different time points.
3. Comparing the abundance of certain bacterial species at three time points between the control and diseased mice as well as within the diseased group.
4. Comparing the counts of Paneth cells between control and diseased mice in relation to dysbiosis resulted from EAE induction.

Chapter 2: Methods

2.1 Animals

Female C57BL/6 mice, with an average weight~20 g at the age of 10-13 weeks were bred and maintained at the animal facility of the College of Medicine & Health Sciences, United Arab Emirates University. Ethical approval to conduct this study was obtained from the Animal Research Ethics Committee of UAE University (Ref. ERA_2021_7326). All mice were housed in sterile polycarbonate cages with free access to food, and water *ad libitum*. Mice were kept in a room maintained at 22-24°C with ~60% relative humidity and 12 h light/dark cycles.

2.2 Induction of EAE

Mice were separated into two groups: control and diseased, 8 mice each. All mice were anesthetized with a mix of 87.5 mg/kg ketamine and 12.5 mg/kg xylazine (Ilium, Australia) given intraperitoneally (i.p). Then, control group received 200 µl of incomplete Freund's adjuvant alone (Sigma-Aldrech, USA) subcutaneously in the back while EAE was induced in the other group by administering 200 µl of recombinant MOG 33-55 peptide (200 µg) (AnaSpec, USA) emulsified in incomplete Freund's adjuvant (IFA) supplemented with 3mg/ml of inactivated *Mycobacterium Tuberculosis* H37Ra (Becton- Dickinson Company, USA) given as subcutaneous injections at the back. This was followed by an intraperitoneal injection of 100 µl pertussis toxin(500 ng) (Sigma-Aldrich, USA) on day 0 and 48 h post-immunization (Wang et al., 2016).

Mice were monitored daily for weight and clinical score evaluation using the following scale; 0: No clinical sign, 1: Flaccid tail (Tail paralysis), 2: Hind limb weakness; 3:

severe hind limb weakness, 4: Complete hind limb paralysis; 5: Death. In the case of mouse death, score 5 was recorded and the mouse was excluded from the study. At advanced stages of the disease starting from score 2, food and water were made closely accessible to mice inside the cage (Hasselmann et al., 2017; Seno et al., 2015).

2.3 Histological Analysis

2.3.1 Processing of Spinal Cord Samples for Histological Analysis

In order to confirm successful disease induction. Mice were anesthetized with ketamine xylazine (Ilium, Australia) followed by transcardial perfusion using 20 ml cold phosphate-buffered saline (PBS) followed by 50 ml of 10% formalin. Spinal cord was flushed out with 10% formalin and placed in the same fixative overnight. After fixation, tissues were washed with PBS three times, 5 min each, then dehydrated in ascending grades of ethanol (50, 70, 80, 90, 95 100 and100%) for 1 hour each on the shaker. Tissues were cleared by placing them in two changes of xylene for 15 min each. Later, tissues were wrapped in lens papers, placed in labeled embedding cassettes and incubated in 3 changes of paraffin at 60°C for 1 h each. Tissues were then embedded in paraffin blocks using the automatic sample preparation system HistoStar™ (Thermo Scientific, USA), placed on the cold plate for 30 min after which, they were allowed to chill overnight. Subsequent trimming and sectioning steps were performed using pfm Rotary 3004 M microtome from pfm medical, Germany to generate sections of 7 and 10 μm thicknesses.

2.3.2 Hematoxylin and Eosin (H&E) Staining

In order to assess levels of mononuclear cells infiltration into spinal cord sections, spinal cord paraffin sections of 7 μm were placed on a hot plate set at 60°C for 1 min

prior staining in order to melt the fat and enhance tissue's adherence to the slide. H & E staining kit (IHC World, USA) was used following the manufacturer's protocol with slight modification. Slides were cleared in 2 changes of xylene for 10 min each at room temperature (RT), after which tissues were hydrated by placing them in descending gradient of ethanol; (2x) 100% for 5 min each, 95% for 2 min, and 70% for 2 min. Slides were later washed briefly with distilled water then stained with hematoxylin for 45 sec followed by 3 quick dips in acid ethanol to remove excess staining. Slides were then placed under slow running tap water for 10 mins, rinsed in distilled water, dipped 10 times in 95% ethanol and were later stained with eosin for 2 min. Finally, sections were dehydrated in 95% ethanol for 5 min, then in two changes of absolute ethanol for 5 min each. This was followed by clearing sections in two changes of xylene for 5 min each. Slides were cover slipped with DPX and were left to dry overnight at RT.

Sections were studied using light microscope to assess the level of mononuclear cell infiltration graded on a scale from 0 to 4 using the following semi-quantitative scoring 0: No inflammation, 1: Cellular inflammation in perivascular area and meninges, 2: Mild: < 1/3 of white matter is invaded by inflammatory cells, 3: Moderate: > 1/3 of white matter is invaded by inflammatory cells, and 4: All white matter is invaded with inflammatory cells (Lukic et al., 2003).

2.3.3 Luxol Fast Blue (LFB) Staining

Spinal cord sections of 10 μm were subject to LFB staining to assess the level of demyelination in spinal cord sections of diseased mice. Staining was performed using LFB staining kit (IHC World, USA) and following the manufacturer's guidance with some modifications. Spinal cord sections were heated at 60°C on a hot plate for 1 min and were then, cleared by incubation in two changes of xylene at RT for 10 min each.

Sections were later hydrated through incubation in two changes of absolute ethanol for 5 minutes each followed by 95% ethanol for 3 min. Sections were then moved into a petri dish containing LFB solution and were placed in an oven at 60°C for 1 hour after which, they were left at RT for +12 hours. Excess LFB stain was rinsed off by dipping slides in 95% ethanol followed by rinsing in distilled water for 1 min. The differentiation step was carried out in the hood where slides were immersed in lithium carbonate solution for 20 sec, rinsed quickly in 70% ethanol for 30 sec then rinsed with distilled water. Differentiation is essential to ensure the removal of excess blue color which was checked under light microscope. In situations where sections are densely stained with blue, differentiation step was repeated. Later, slides were placed in distilled water then counterstained in cresyl violet for 1–2 min then rinsed with distilled water. Sections were transferred into varying concentrations of ethanol 95%, 100%, and 100% ethanol for 5 min each. Slides were later placed in 2 changes of xylene for 5 min each, after which they were cover slipped with DPX and left overnight at RT to dry.

Sections were analyzed under light microscopy and the assessment of demyelination was done by estimating the percentage of the demyelinated area by a histopathologist. Cresyl violet stained neurons violet and LFB solution-stained myelin with blue-green color, loss of stain in some areas is an indication of demyelination.

2.4 Lectine Histochemistry (Intestine)

Histochemistry staining with lectin was used to visualize Paneth cells located at the bottom of the crypts that is responsible for the control of gastrointestinal flora (Lueschow & McElroy, 2020). Mice from both groups were sacrificed at the end of the experiment (n=3 from each group).

2.4.1 Intestinal Tissue Processing

Mice from control and diseased group were anesthetized with ketamine-xylazine then cardiac perfusion was performed with 20 ml cold PBS. Two segments were collected from the intestine: 2 cm from the pyloric end of the stomach (Called duodenum) and 2 cm before the cecum (Ileum). Segments were placed on a Petri dish filled with paraffin and pinned with needles. Boiun's fixative (composed of picric acid, formaldehyde, and acetic acid) was applied on the stretched tissue and was left for 10 min before moving it to a tube containing the same fixative and was incubated overnight. After fixation, tissues were dehydrated in an ascending grades of ethanol (70,80, 90, 95 100 and100%) 1 hour each followed by clearing in xylene twice for 15 min each. Tissues were moved into labeled embedding cassettes and incubated in 3 changes of paraffin for 1 h each at 60°C. Tissues were later embedded in paraffin blocks using the automatic sample preparation system HistoStar™ (Thermo Scientific, USA) then, placed on the ice plate for 30 min and were left to dry overnight at RT. Paraffin tissue sections of 7 μm thicknesses were prepared and collected on a gelatin-coated slides and were left to air dry.

2.4.2 Lectin Staining

Lectin staining was performed to specifically label and quantify Paneth cells in the control (n= 3) and diseased mice (n= 3). Proper adherence of the tissue sections was achieved by placing the slides on a hot plate at 60°C for 1 min and then deparaffinized in jars containing two changes of xylene for 5 min each. This was followed by hydrating intestinal sections by incubation in two changes of 100% ethanol for 5 min each and later in 95%, 90%, 70%, 50% ethanol for 3 min each. Following hydration, PAP Pen (Abcam, USA) was used to encircle the tissues to ensure that the reagents do

not spill over the slide. Washing with PBS was followed by the application of PBS containing 1% cold bovine serum albumin (BSA) for 45 min. Ulex Europaeus agglutinin I (UEA I) conjugated to fluorescein isothiocyanate (FITC) (Thermo Fisher, USA) was later applied on the tissues at a dilution of 1:1000 in 1% cold BSA to label Paneth cells. The staining was performed in dark for 1 h followed by washing with PBS to remove excess lectin and tissues on slides were later mounted with 50% glycerol. Slides were kept at 4°C until visualization using the confocal microscope.

Images at 40x were captured by confocal microscope. Both total count of Paneth cells and labeled intensity from both intestinal segments were averaged from each mouse per analyzed crypt. Three tissue sections per mouse were assessed and labeled Paneth cells in 10 longitudinally cut crypts were examined. Cells counts were estimated manually using the manual cells counting on ImageJ. For the estimation of lectin labeling intensity in each crypt, squares were drawn around one crypt of control mouse and then the integrated density (The sum of pixels within the selected area) was determined automatically using the analysis tools. Squares of the same size were dragged across all samples to measure intensity in the same area of the control. The values obtained represent the amount of lectin in the analyzed crypts. Values were transferred to Excel to compute the fold change.

2.5 Flow Cytometry

All fluorescence activated cell sorting (FACS) antibodies used were purchased from (BioLegend, USA), including: Anti-$CD8^+$a (53-6.7, APCCy7-conjugated), anti-NK-1.1 (PK136, FITC-conjugated), anti-CD314 (NKG2D) (CX5, APC-conjugated), anti-CD159a (NKG2AB6) (16A11, PE-conjugated), anti-CD3 (17A2, Brillant Violet 421-conjugated), anti-$CD4^+$ (RM4-5, Brilliant Violet 785-conjugated), and anti-$CD45^+$

(30-F11, Brilliant Violet 605-conjugated. For FACS analysis, the BD FACS Celesta instrument (BD Biosciences, Germany) was used, and FlowJo software (FlowJo, LLC, USA) was used for data analysis.

2.5.1 Isolation and Flow Cytometry Analysis of Circulating Lymphocytes

2.5.1.1 Reagents

Lysis buffer was prepared by combining 7.7 g NH4Cl, 0.1 g, KHCO3, 1L distilled water. Buffer was sterilized by passing it through 0.22 µM pores filter.

FACS buffer composed of 100 ml PBS, 5 ml FBS, and 0.1 g sodium azide (NaN_3).

2.5.1.2 Procedure

Blood samples were collected from control (n=10), diseased- score 1 (n=6), and diseased-peak (n=9) mice by cardiac puncture after anesthetizing mice with a mix of 87.5 mg/kg ketamine and 12.5 mg/kg xylazine. 200-400 µl of blood was collected in an EDTA tube and later transferred to a 50 ml conical tube containing RBCs lysis buffer and incubated for 5 minutes (1 ml of RBCs lysis buffer is added to each 100 µl of blood). Lysis reaction was blocked by the addition of 20 ml of cold PBS followed by 8 min centrifugation at 4°C, 1400 rpm. Supernatant was then discarded and the RBCs lysis step was repeated for the samples where the RBCs were not completely lysed. Pellet was resuspended with 1 ml of PBS 5% FBS. Prior to staining, cell suspension was transferred to FACS tubes, centrifuged again for 5 min at 4°C, 1400 rpm, and the supernatant was discarded then 50 µl of the antibodies cocktail (diluted in FACS buffer) was added to each tube and incubated for 25 min at 4°C away from light. Cells were then washed with PBS 5% FBS and centrifuged for 5 min at 4°C,

1400 rpm. The supernatant was discarded and 300 µl of FACS buffer was added to the cells. Tubes were kept on ice for analysis.

2.5.2 Isolation and FACS Analysis for Lymphocytes in the IELs

2.5.2.1 Reagents and Media

Harvest media: 475 ml RPMI 1640, 25 ml heat-inactivated FBS, and 5 ml 100× HGPG (Stored at 4°C).

10X HEPES-bicarbonate buffer: 23.8 g HEPES, 21 g NaHCO3, 1 L autoclaved H_2O. Solution was filtered using a 0.45 µm filter, pH was adjusted periodically to 7.2 using HCl (stored at RT).

100X HGPG: 59.6 g HEPES, 14.6 g L-glutamine, 1×10^6 U penicillin (2,000 U/ml final), 1 g streptomycin, 2.5 mg gentamicin, 500 ml RPMI 1640. Solution was filtered using a 0.45 µm filter, pH was adjusted to 7.5 using NaOH. Solution was aliquoted and stored at -20°C.

Dithioerythritol (DTE) solution (40 ml/small intestine): 4 ml 10× Hanks balanced salt solution, Ca^{2+}- and Mg^{2+} -free, 4 ml 10× HEPES-bicarbonate buffer, and 4 ml heat-inactivated FBS, 6.16 mg dithioerythritol, and 28 ml autoclaved H_2O. DTE was freshly prepared for each experiment.

1X density gradient (DG) stock solution: 90 ml Percoll and 10 ml 10X PBS (stored at 4°C).

44% DG solution (8 ml/small intestine): 3.52 ml 1× DG stock solution, and 4.48 RPMI 1640 (freshly prepared).

67% DG solution (5 ml/intestine): 3.35 ml 1× DG stock solution, and 1.65 RPMI 1640 (freshly prepared).

2.5.2.2 Procedure

A modified protocol from the Journal of Visualized Experiments (JOVE) Qiu & Sheridan (2018) was used in this experiment to assess the level of $CD4^+$, $CD8^+$ T cells, and NK cells and the number of cells expressing of activating and inhibitory receptors from the intestine specifically IELs. Transcardial perfusion using 20 ml cold PBS was performed to wash out feces and circulating cells from the intestine. To extract the small intestine, the stomach, cecum, fat and MLNs were identified and removed. The small intestine was placed and rolled on a thick paper towel to remove blood and fat. Intestinal tissues were kept moist with cold harvest media. Peyer's patches were removed with a curved scissor, while stool and mucus were expelled twice by sliding forceps from the duodenum towards the ileum. A small-sized scissor was used to cut through the small intestine, then into 2 cm pieces. Intestinal pieces were placed in a 50 ml conical tube containing 20 ml cold harvest media and stored on ice for further processing.

Intestinal pieces were washed with 25 ml of cold harvest media by inverting the tube slowly ten times and later, supernatant was discarded. This step was repeated three times (The intestinal pieces should settle in the bottom of the tube each time to ensure the removal of fat and MLNs). Washing steps were followed by the addition of 20 ml of freshly prepared prewarmed Dithioerythritol (DTE) solution to the intestinal pieces which were later transferred to a 150 ml glass Erlenmeyer flask. The Erlenmeyer flask containing the intestinal pieces was placed on a stirrer for 20 min at 37°C, 220 rpm. Following incubation, intestinal pieces in DTE were transferred to a new 50 ml conical

tube, vortexed at high speed for 10 sec then supernatant was poured into a new 50 ml conical tube through a 70 µm cell strainer with ensuring that tissue pieces remain in the original tube. The supernatant, containing the IELs, was centrifuged at 1400 rpm at 4°C, for 8 min. Supernatant was removed and pellet was resuspended with 10 ml cold harvest media and stored on ice for later processing. The same previous steps for isolation of IELs were repeated to ensure isolation of as many IELs as possible from remaining intestinal pieces by adding 20 ml DTE solution and incubation on a stirrer at 37°C, 220 rpm for another 20 min. Same subsequent steps were repeated. Flask compartments were transferred to a new 50 ml conical tube, vortexed, and strained into the tube containing the supernatant from the previous incubation. Tubes were then centrifuged at 4°C, 1400 rpm for 8 min and the pellet was resuspended with 8 ml of freshly prepared 44% DG solution at RT. 5 ml of freshly prepared 67% DG solution at RT was added to a 17 mm ø x 100 mm 14 ml polypropylene round-bottom tube, then was gently overlaid with the 8 ml 44% DG solution/cell suspension using a pipette gun. Tubes were centrifuged at RT, 2000 rpm for 20 min without break (acceleration =1 | deceleration= 1). After centrifugation, the top part containing dead cells and epithelial cells was removed by a Pasteur pipette and the cells of interest in the interface were harvested and placed in a 50 ml conical tube containing 40 ml cold harvest media. Cells were pelleted by centrifugation at 4°C, 1400 rpm for 8 min and later were resuspended with 1 ml cold harvest media. Prior to staining, cell suspension was transferred to FACS tubes, centrifuged again for 5 min at 4°C, 1400 rpm, and the supernatant was discarded and replaced with 50 µl of antibodies cocktail (diluted in FACS buffer) added to each tube and incubated for 25 min at 4°C protected from light. Cells were then washed with cold PBS 5% FBS and centrifuged for 5 min at 4°C, 1400

rpm after which supernatant was discarded, and pellet was resuspended in 300 µl of FACS buffer, and tubes were kept on ice for analysis.

2.6 Detection and Quantification of Selected Gut Microbes

2.6.1 Sample Collection

Feces were collected from control (n=5), diseased-score 1 (n=6) mice, and diseased-score 2-3 (n=6) mice twice at each time point; at the baseline, disease onset, and the peak (Score 2-3) and at relative time points in the control group. One mouse died from the control group before the sample collection at the third time point which was excluded from the study. From control mice (n=5), stool samples were collected at the baseline, onset, and peak. Only samples at the baseline and onset were collected for the mice sacrificed at the onset of the disease (n=6). As for diseased-peak mice (n=6), samples were examined at the baseline and peak only. The collection of the samples was performed by holding up the mice and placing a sterile Eppendorf tube (1.5 ml) at the anal canal where they smoothly defecate. The samples were immediately stored at -80ºC until processing.

2.6.2 DNA Extraction

Total DNA was purified from the stool using QIAamp Fast DNA Stool Mini Kit (Qiagen, Germany) following the manufacturer's protocol and was modified to reach the maximum DNA concentration. Collected stool sample (>100 mg) was weighed and 400 µl from of inhibiEX buffer was added per 100 mg of stool. Samples were mixed with the buffer using a sterile stick and then vortexed until homogenized. After that, samples were incubated at 95°C, 400 rpm for 15 min then vortexed at maximum speed for 15 sec and centrifuged at RT, 14,000 rpm for 2 min. During that time, 15 µl

of proteinase K was added to labeled Eppendorf tubes, supernatant from the centrifugation were then added to the tubes containing proteinase K followed by 200 µl of buffer AL and vortexed again for 15 sec at the maximum setting. Samples were later incubated at 70°C for 10 min after which, 200 µl of absolute ethanol was added to the mix and vortexed. After adding the ethanol, the whole sample was added to the labeled QlAamp spin columns, and were centrifuged for 1 min at RT, 14,000 rpm. QlAamp columns were placed in a new 2 ml tube and the filtrate was discarded. Buffer AW1 (500 µl) was added to the column then columns were centrifuged at the maximum speed for 1 min, at RT. Following centrifugation, tube containing filtrate was discarded and the QlAamp was placed in a new 2 ml tube with 500 µl of buffer AW2 added followed by centrifugation for 6 min, RT, 14,000 rpm. In preparation for the binding step, QIAamp columns were transferred into a new labeled 1.5 ml Eppendorf tube, then 40 µl of the buffer ATE (Elution buffer) was pipetted directly on the filter and incubated at RT for 2 min. DNA samples were eluted by centrifuging columns for 2 min at RT, 14,000 rpm. The elution step was repeated twice for each sample to obtain the maximum amount of DNA from each sample.

2.6.3 Real-Time PCR

RT-PCR was performed for the detection and quantification of the following selected gut microbes: *Lactobacillus reuteri*, *Prevotella copri*, *Bacteroides fragilis*, *Clostridium perfringens*, and *Akkermansia muciniphila*, at 3 different time points through the course of disease in both mice groups. All primers were purchased from (Gene link/ e-oligos, USA) and their sequences are listed in Table 1. All primers specificity was confirmed by conventional PCR.

Table 1: The sequences of primers for RT-PCR

Target	Sequence	Reference
16SRNA (Housekeeping gene)	F: TCCTACGGGAGGCAGCAGT	(Hopkins et al., 2005)
	R: GGACTACCAGGGTATCTAATCCTGTT	
Lactobacillus reuteri	F: GAGAGCCTGCTATATGCCAGC	(Egervärn et al., 2009)
	R: GGGCGTATCCACAATGTTAAC	
Prevotella copri	F: CCGGACTCCTGCCCCTGCAA	(Verbrugghe et al., 2021)
	R: GTTGCGCCAGGCACTGCGAT	
Bacteroides fragilis	F: CACTTGACTGTTGTAGATAAAGC	(Papaparaskevas et al., 2013)
	R: CATCTTCATTGCAGCATTATCC	
Clostridium perfringens	F: GGGGGTTTCAACACCTCC	(Nagpal et al., 2015)
	R: GCAAGGGATGTCAAGTGT	
Akkermansia muciniphila	F: CAGCACGTGAAGGTGGGGAC	(Earley et al., 2019)
	R: CCTTGCGGTTGGCTTCAGAT	

Real-Time -PCR was carried using 5X HOT FIREPol® EvaGreen® qPCR Supermix (Solis BioDyne, Estonia). Briefly, 4 µl of 5x hot FIREPol EvaGreen qPCR supermix was added to a labeled Eppendorf tube containing 13.2 µl of RNase/ DNase free water and 0.4 µl of forward and reverse primers with a concentration of 10 µM. Then, 18 µl of each mix was added to each well of 96-well PCR plate (Applied Biosystems, USA) followed by 2 µl of the desired DNA. All samples were tested in duplicate.

The reactions were run using 7500 Real Time PCR system (Thermo Fisher Scientific, USA) with the following cycling steps:

- Initial activation, 95°C for 12 min
- Denaturation at 95°C for 15 sec
- Annealing at 60°C for 30 sec
- Elongation at 72°C for 30 sec

X 40 cycles

Melts curves shown in Figure 4 were used to assess whether the amplifications were true or non-specific by comparing the melting temperature of each positive sample to its negative control. Almost same melting temperatures indicate non-specific amplification. The data was analyzed using 7300 Real-Time PCR System Software v1.4.1 (Applied Biosystems, USA), then exported to Microsoft Excel for further analysis. Samples with a difference of >1 cycle between the duplicates were repeated. The housekeeping gene was the bacterial 16S rRNA gene that was used for normalization to obtain ΔCt value. This value was used to calculate the ΔΔCt (ΔCt of the sample- avg ΔCt of the control or baseline). Fold change was then obtained by the following equation = $2^{\wedge -\Delta\Delta Ct}$. Statistical analysis was performed using GraphPad prism.

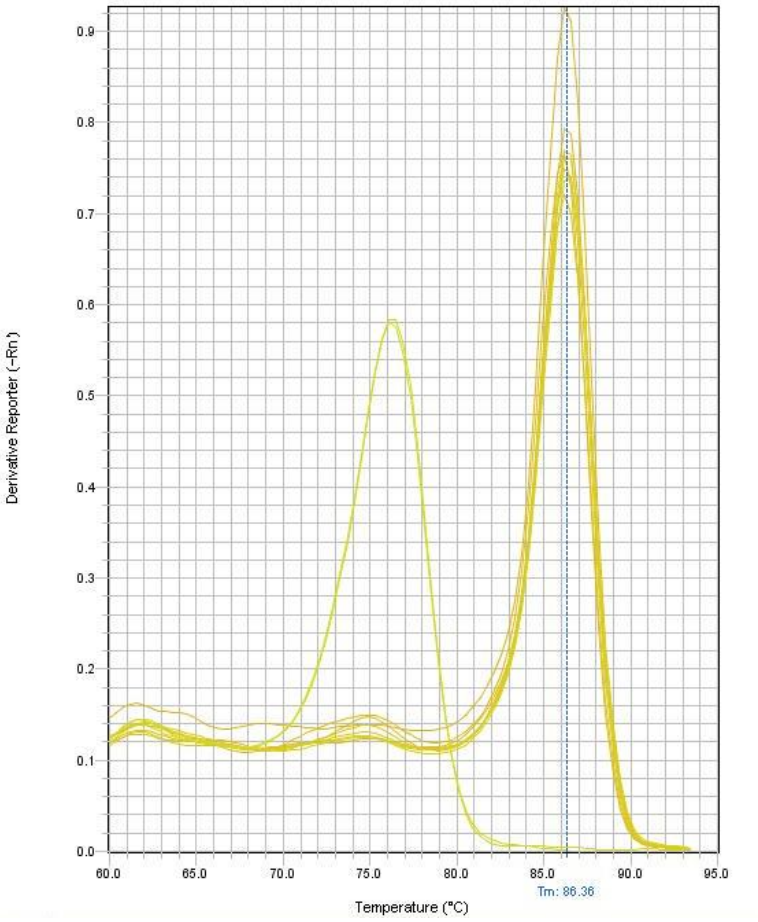

Figure 4: Melt curve illustrating negative control and positive samples for the determination of the true amplifications.

2.7 Statistical Analysis

All statistical analyses were performed on GraphPad prism using Mann-Whitney U test for the comparisons between independent variables. Two-tailed Spearman's test was used for correlation analysis which was performed on SPSS (Version 26, IBM SPSS® Statistics, USA). The total count of Paneth cells and raw integrated density were measured on ImageJ software. A p value less than 0.05 was used to define statistical significance.

Chapter 3: Results

3.1 Successful Induction of EAE in C57BL/6 Female Mice

EAE was induced in female C57BL/6 mice as previously described and a group injected with IFA served as a control. Mice were evaluated daily for their weight and clinical scores for approximately 20 days starting from the second shot of PTX. Average starting weight of all mice was ~20 g. Changes in body weight were reported daily and calculated as percentages, compared to the starting weight (Figure 5A). The control group showed normal and steady increase in their body weight compared to diseased mice where significant weight loss was reported starting within the first 7 days following disease induction. The weight loss continued until the end of the study ($P<0.0001$). The average weight loss of the immunized mice at the onset (Score 1) was roughly 6% of the total body weight and 18% when they reached the peak (Score 3) of the disease.

Most diseased mice in both experiments showed their first symptom, the weakness of the tail, on day 11, and 2-3 days later, they reached score 3, partially paralyzed (Figure 5B) ($P=0.0058$). In fact, 3 mice showed tail paralysis on day 11, 2 mice on day 12, and 4 mice on day 16. Mice normally shows different responses to the induction due to their genetic predisposition, approximately 20% of the mice were resistant to the disease and others did not reach the peak; these were excluded from the study. Mice in the control group remained asymptomatic (score 0) throughout the 20 days by which all the group was sacrificed.

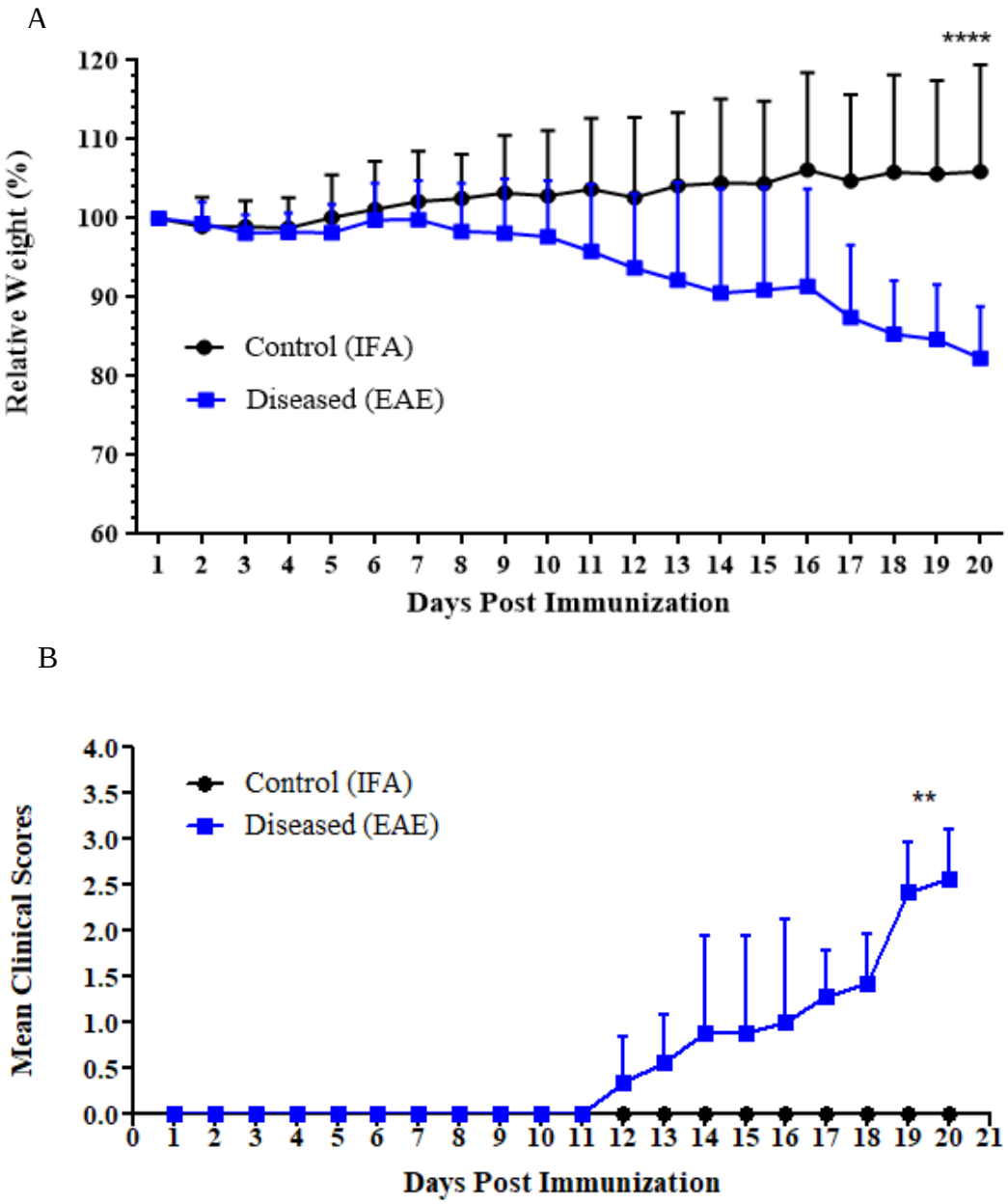

Figure 5: Change of body weight and scores during the course of EAE. Control mice (n=10) received incomplete Freund's adjuvant and diseased mice (n=9) were immunized with MOG35-55 and 2 shots of PTX. (A): The relative weight change for control and diseased mice along 20 days. (B): The mean clinical score of control and diseased mice along 20 days. Results are combined from two independent experiments and expressed as mean ± SD. Mann–Whitney U test was performed to determine P values (** $P \leq 0.01$, **** $P \leq 0.0001$).

3.2 Histological Assessment of Infiltration Level of Mononuclear Cells and Demyelination in the Spinal Cords of Control and Diseased C57BL/6 Mice

Level of mononuclear cellular infiltration into spinal cords was assessed through H&E staining of spinal cord sections in both control and diseased mice. Spinal cord specimens from control (n=3) and diseased mice (n=4) were processed and stained with H&E at the end of the experiment. More than 3 sections from each mouse were examined for cellular infiltration. Semi-quantitative assessment of H&E stained spinal cord sections of diseased mice showed very intense infiltration of mononuclear cells with perivascular cuffing (Score 4) compared to the control group showing no infiltration (P=0.003) (Figure 6A, B, & C). The highest given cell infiltration score was 4 for a mouse that was reported as clinically score 3 (Figure 6D, E, & C).

As for demyelination, the average percentage of areas of demyelination in the white matter of examined sections using LFB staining (Figure 6F, G) showed 38% estimated area of demyelination in stained sections of the diseased group (Figure 6I, J, & H) compared to 10% in the control (P=0.04) (Figure 6H). The highest percentage was 90-100% demyelination for a score 3 mouse and the lowest demyelination was observed in score 1 mouse with 20-25% demyelination in the diseased group.

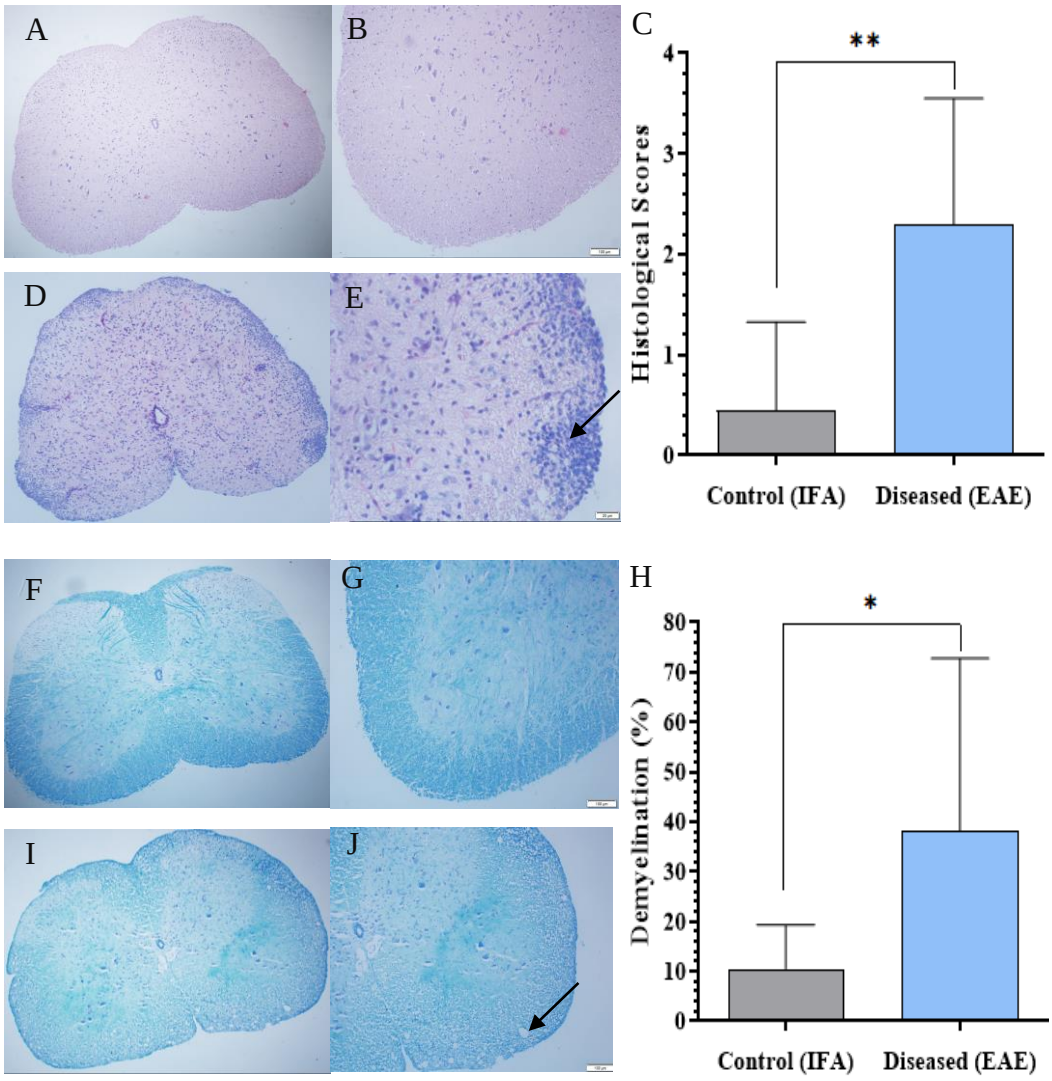

Figure 6: Level of mononuclear cells infiltration and demyelination among control (n=3) and EAE immunized mice (n=4) assessed by H&E and LFB staining. (A, B): H&E stained spinal cord sections from control mice. (D, E): H&E stained spinal cord sections from diseased mice showing the infiltration of the mononuclear cells. (C): A semi-quantification of the histological score between the control and diseased mice. (F, G): LFB stained spinal cord sections from control mice. (I, J): LFB stained spinal cord sections from diseased mice showing the demyelinated areas. H: Assessment of the demyelination by estimating the percentages of the demyelinated area in control and diseased mice. Results are presented by mean ± SD. Mann–Whitney U test was performed to determine P values (* P≤0.05, ** P≤0.01). A, D, F, I Bar=200 µm/ 10x magnification | B, E, G, J Bar=100 µm/ 40x magnification.

3.3 Flowcytometry Analysis for $CD4^+$, $CD8^+$ T Cells and NK Cells in the Circulation and Intestines

The gating strategy described in Figure 7 was used for all groups to determine the frequency of $CD4^+$, $CD8^+$, and NK cells out of the total lymphocytes. In addition, median florescence intensity (MFI) was calculated to assess the level of cells expressing inhibitory (NKG2A) and activating (NKG2D) receptors from the total gated NK cells in the circulation and intestines. Blood and intestine samples were collected and processed as previously described. Samples from control mice were processed for FACS analysis at the end point (day 20), from diseased mice at the onset when they show tail paralysis (At score 1, reached around day 11) and from diseased mice that reached the peak of disease (At score 3, around day 20) characterized by their partial paralysis and loss of control of one of their hind limbs. Mice were sacrificed 24 hours after observing their symptoms to ensure the accuracy of the reported clinical score.

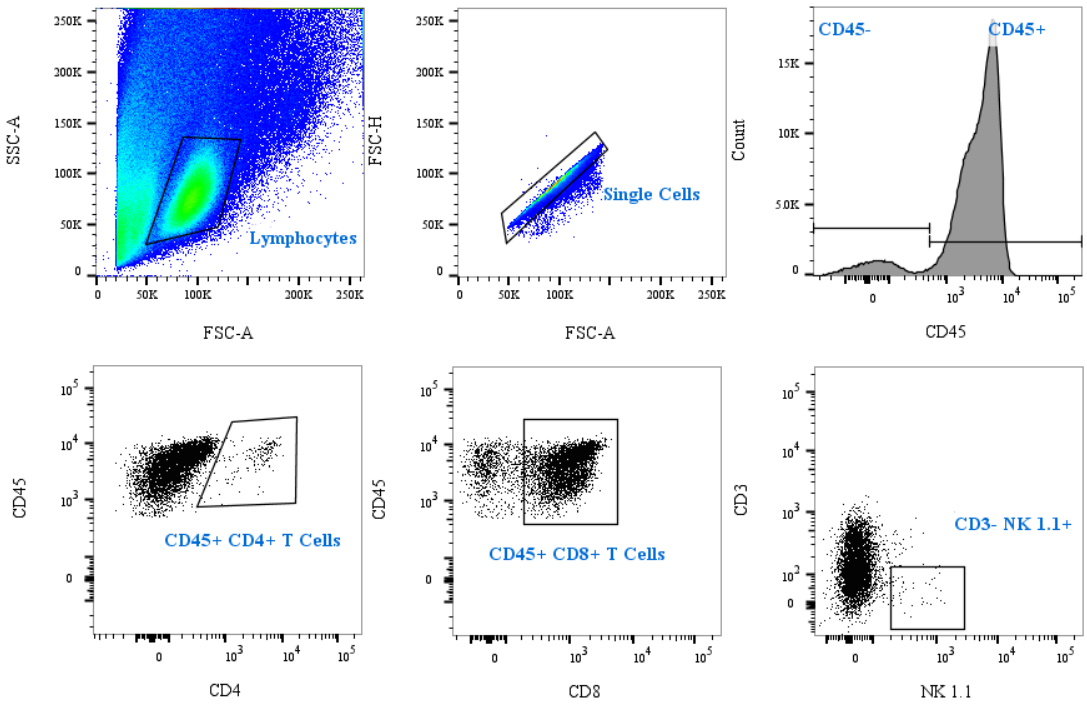

Figure **7**: Flow cytometry gating strategy for lymphocyte populations. Single-cell suspension was prepared from blood and intraepithelial lymphocytes (IEL), compartments were stained with the following fluorescent-labeled antibodies: CD45 for the identification of lymphocytes, total CD4 T cells, CD8 for cytotoxic T cells, and NK 1.1 and CD3 for Natural Killer cells. Gate 1 showed forward scatter (FSC-A) and side scatter (SSC-A) properties. Gate 2 identified single cells from the total lymphocytes. Gate 3 identified hematopoietic cells. Gate 4 showed $CD4^+$ T cells. Gate 5 showed $CD8^+$ T cells. Gate 6 presented NK cells.

3.3.1 Assessment of the Frequencies of $CD4^+$ and $CD8^+$ T Cells in the Circulation and Intestinal Samples at Baseline, Onset and Peak of Disease

$CD4^+$ T cells are the main contributors to the neuroinflammation and the production of proinflammatory cytokines. In the blood, level of $CD4^+$ T cells was estimated as 16.6% of total lymphocytes in the control group and a similar frequency was reported for $CD8^+$ T cells reaching 14.3%. At the disease onset, frequency of $CD4^+$ T did not change significantly compared to its increase at the peak of the disease reaching 37.7% of the total lymphocytes compared to control group ($P<0.0001$). The change in $CD4^+$ T cells frequency between onset and peak was also significant ($P=0.0007$). In

comparison, no change was detected at the three time points for $CD8^+$ T cells frequencies (P>0.05) (Figure 8).

Frequencies of $CD4^+$ and $CD8^+$ T cells were assessed by FACS in harvested IELs. $CD8^+$ T cells were found to make the majority (70%) of total lymphocytes in the control mice and only 5-10% were $CD4^+$ T cells. Variations in the frequencies of $CD8^+$ and $CD4^+$ T cells were similar to the reported results of circulating lymphocytes. $CD8^+$ T cells frequency remained unchanged in the 3 time points (P>0.05). While the slight increase of $CD4^+$ T cells at the onset and peak were not statistically significant (P>0.05) (Figure 9).

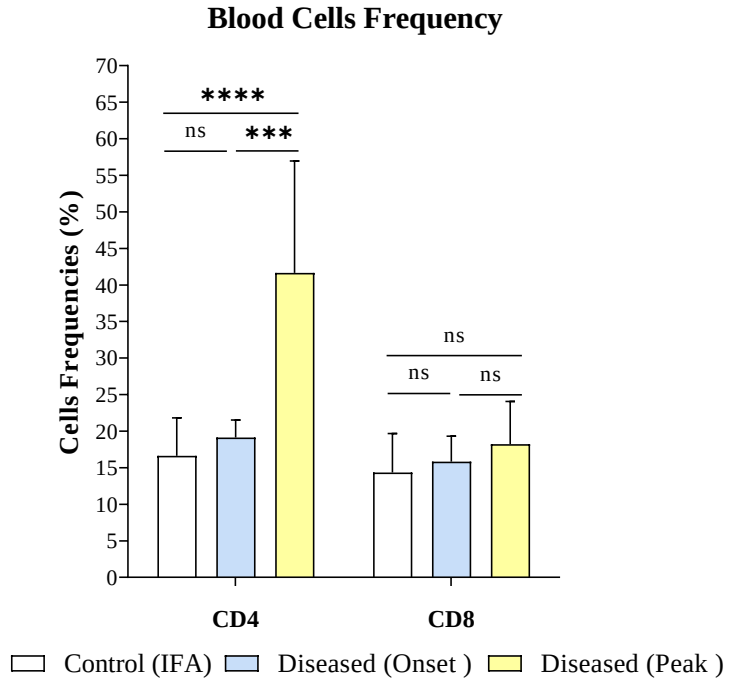

Figure 8: Average frequencies of $CD4^+$ and $CD8^+$ T cells in the circulation of control (n=10), diseased-onset (n=6), and diseased-peak (n=9) mice. Results are combined from two independent experiments and expressed as mean ± SD. Mann–Whitney U test was performed to determine P values (*** P≤0.001, **** P≤0.0001, ns P>0.05).

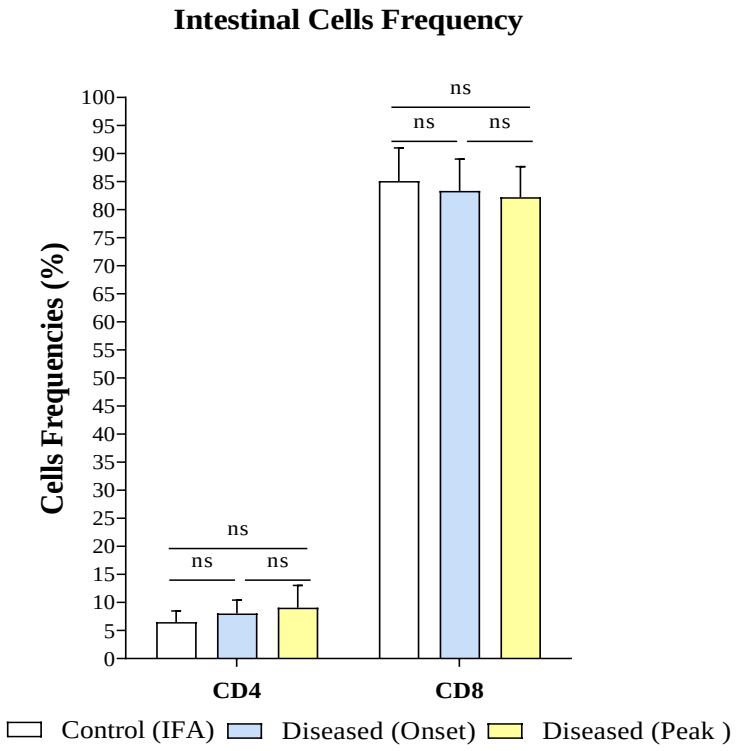

Figure 9: Average frequencies of $CD4^+$ and $CD8^+$ T cells in control (n=10), diseased-onset (n=6), and diseased-peak (n=9) mice IELs. Results are combined from two independent experiments and expressed as mean ± SD. Mann–Whitney U test was performed to determine P values (ns P>0.05).

3.3.2 Frequencies of Circulating and Intestinal NK Cells

Figure 10A, demonstrated a significant increase in the frequency of circulating NK cells at the disease onset (P=0.002), but later decrease at the peak of disease (P=0.0360). This change was significant compared to the frequency at the onset (P=0.0360), but not when compared to the control mice. The mean frequency of NK cells in the blood was 3.2% for control mice, 11.2% for the diseased mice at score 1, and 6.39% at the peak of the disease.

Frequency of NK cells in the gut did not change between the control group (1.9%) and the disease onset (2.04%). Percentage of NK cells significantly increased at the peak of the disease to 5.24% compared to both disease onset and control (P=0.0176 and 0.0010, respectively) (Figure 10B).

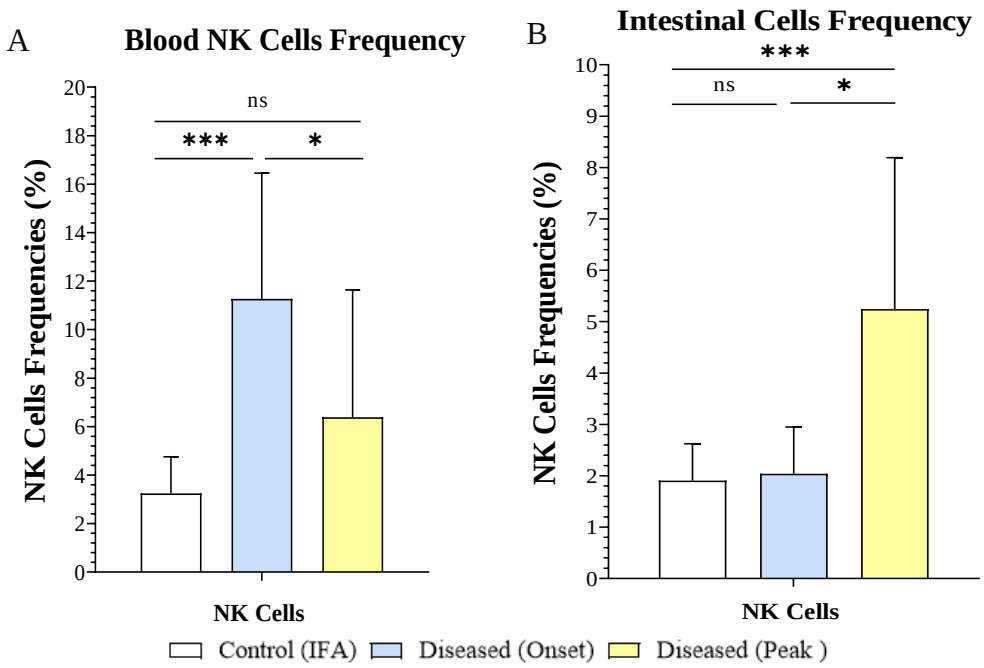

Figure 10: Average frequency of circulating and gut NK cells in control (n=10), diseased-onset (n=6), and diseased-peak (n=9) mice. (A): Frequency of circulating NK cells. (B): Frequency of gut NK cells. Results are combined from two independent experiments and expressed as mean ± SD. Mann–Whitney U test was performed to determine P values (* P≤0.05, *** P≤0.001, ns P>0.05).

3.3.2.1 Assessment of the Activity Level of NK Cells through Detecting Expression of Activating (NKG2D) and Inhibitory (NKG2A) Receptors on Circulating and Gut NK Cells

MFI of NKG2D was significantly downregulated almost to the half (100.7 AU) (P=0.0225) at the onset compared to the control, followed by a non-significant increase

at the peak to 804.1 AU (P>0.05). Changes in the expression of NKG2A were not statistically significant though (P>0.05) (Figure 11).

In the intestine (Figure 12), the control mice showed high MFI of NKG2D (117.7 AU) that was significantly downregulated at the onset to 45.5 AU (P=0.0017) and upregulated when mice reached peak of the disease (P=0.0007) and this increase was statistically significant in comparison to the onset but not to the control group. As for NKG2A, similar to its expression on circulating NK cells, no statistically significant change was reported between the groups.

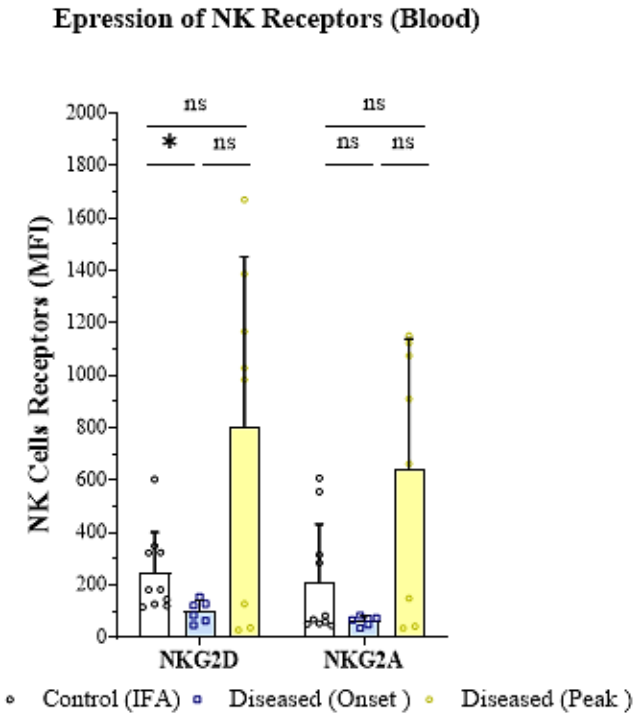

Figure 11: Average MFI of NKG2D and NKG2A on circulating NK cells in control (n=10), diseased-onset (n=6), and diseased-peak (n=9) mice. Results described are combined from two independent experiments and expressed as mean ± SD. Mann–Whitney U test was performed to determine P values (* P≤0.05, ns P>0.05).

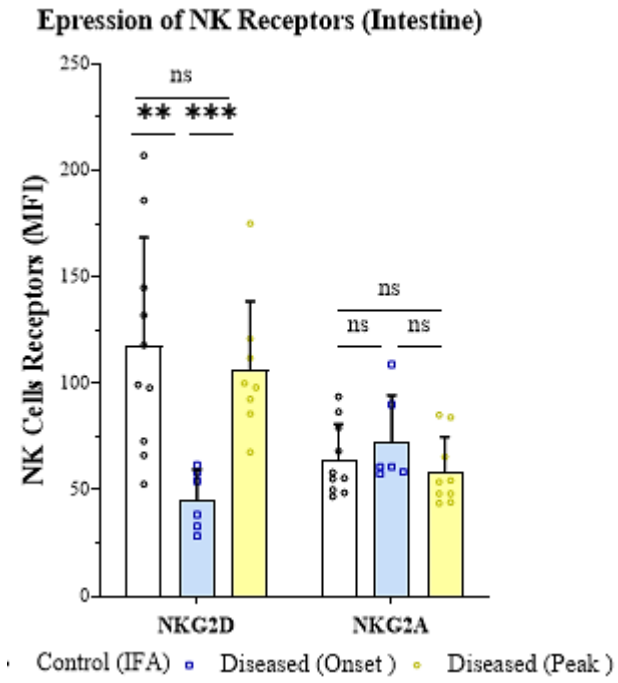

Figure 12: Average MFI of NKG2D and NKG2A on intestinal (IELs) NK cells in control (n=10), diseased-onset (n=6), and diseased-peak (n=9) mice. Described results are combined from two independent experiments and expressed as mean ± SD. Mann–Whitney U test was performed to determine P values (** P≤0.01, *** P≤0.001, ns P>0.05).

3.4 Correlation of Gut $CD4^+$, $CD8^+$ T Cells, and NK Cells

Spearman's r was computed to highlight the correlation between the immune cells in the intestine. There was a significant negative correlation between the frequencies of $CD4^+$ and $CD8^+$ T cells (r=-0.485 P=0.035). Additionally, the association between $CD4^+$ T cells and NK cells is positively correlated with a r value equal to 0.435. While the correlation between $CD8^+$ T cells and NK cells is weakly negative (r=-0.248) (Table 2). These data indicate that increase in the percentage of $CD4^+$ in the gut is correlated with the increase in the percentage of NK cells and decrease of $CD8^+$ T cells.

Table 2: Association between the immune cells isolated from the gut (IELs)

			iCD4$^+$	**iCD8$^+$**	**iNK**
Spearman's rho	**iCD4$^+$**	r		-0.485*	0.435
		P-value		0.035	0.063
	iCD8$^+$	r	-0.485*		-0.248
		P-value	0.035		0.305
	iNK	r	0.435	-0.248	
		P-value	0.063	0.305	

*. Correlation is significant at the 0.01 level (2-tailed).

3.5 Microbiota Changes during EAE when Normalized to the Control Group

Analysis of the changes in the tested bacterial species was performed on the collected stool samples from control, diseased-onset, and diseased-peak groups. qPCR was applied to examine the fold change of the following bacteria: *Akkermansia muciniphila, Bacteroides fragilis, Lactobacillus reuteri, Prevotella copri,* and *Clostridium perfringens. A. muciniphila and B. fragilis* were below the detection limit in all mice at all time points. *L. reuteri and P. copri* were found in all mice at all stages of EAE whereas *C. perfiengens* was found only in 2 mice among the diseased-peak group.

Figure 13 (A & B) describes the difference in *L. reuteri* and *P. copri* between the control and diseased groups. There was a variation in the results yet, the mean fold change of *L. reuteri* was reduced, but not significant between the diseased-onset compared to the control group. While it was significantly reduced to 0.3 in the diseased-peak group compared to the control (2.1) (P=0.0192), but not to the disease onset (0.6) (Figure 13A). As for *P. copri*, their abundance was reduced insignificantly in the diseased-onset mice and reduced more in the diseased-peak group where the fold

change was below 1 for most of the mice; this reduction is significant in comparison to the control group (P=0.0087), but nearly significant compared to the onset (P=0.0519) (Figure 13B).

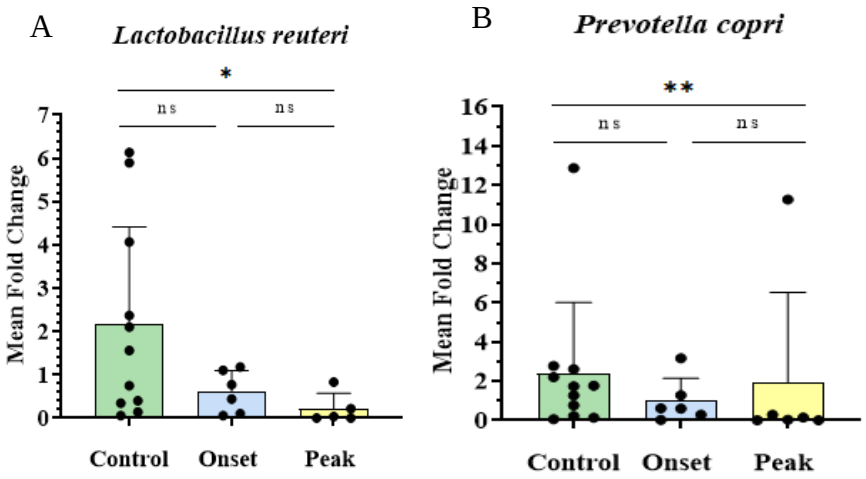

Figure 13: Mean Fold change of *L. reuteri* and *P. copri*, in control (n=5), diseased-onset (n=6), and diseased-peak (n=6). (A): Mean fold change of *L. reuteri* among the three groups. (B): Mean fold change of *P. copri* between the three groups. All results are expressed as mean ± SD. Mann–Whitney U test was performed to determine P values (*P≤0.05, **P≤0.01, ns P>0.05).

3.6 Microbiota Changes during EAE when Normalized to the Baseline

Same samples were analyzed and normalized to the baseline of each mouse to obtain the change of the species in the same mouse throughout the whole experiment.

3.6.1 *Lactobacillus reuteri*

No significant change was found in the abundance of *L. reuteri* among the control group at the three time points. (Figure 14A). Figure 14C shows that the overall fold change of *L. reuteri* did not significantly changed; four mice retain the fold change at the onset while two of them showed increase causing overall increase in the abundance of this species. In comparison to mice at the peak of disease (Figure 14E), the average

fold change at the peak was 0.4 which was significant compared to the baseline (P=0.0476), although one mouse of that group showed an increase in the fold change at that time point.

3.6.2 *Prevotella copri*

Similar to *L. reuteri*, the abundance of *P. copri* in the control group did not change among the three time points (Figure 14B). Figure 14D illustrates the variation in the mean fold change at the onset compared to the baseline making the difference non-significant. These results are opposing the results of the mice that reached score 3 (Figure 14F), as the fold change of all mice was below 1 except for one mouse that showed fold increase to 6 at the peak of the disease. Despite that the SD of the fold change was high at the peak, the change was statistically significant (P=0.0476).

3.6.3 *Clostridium perfringens*

Mice receiving adjuvant showed negative results to *C. perfringens* and only 2 mice out of 6 that reached score 3 showed positive results to this specie. Data presented in Figure 14G showed that the average fold change increased insignificantly. Indeed, one mouse showed an increase of this bacteria while the other one showed contradictory results.

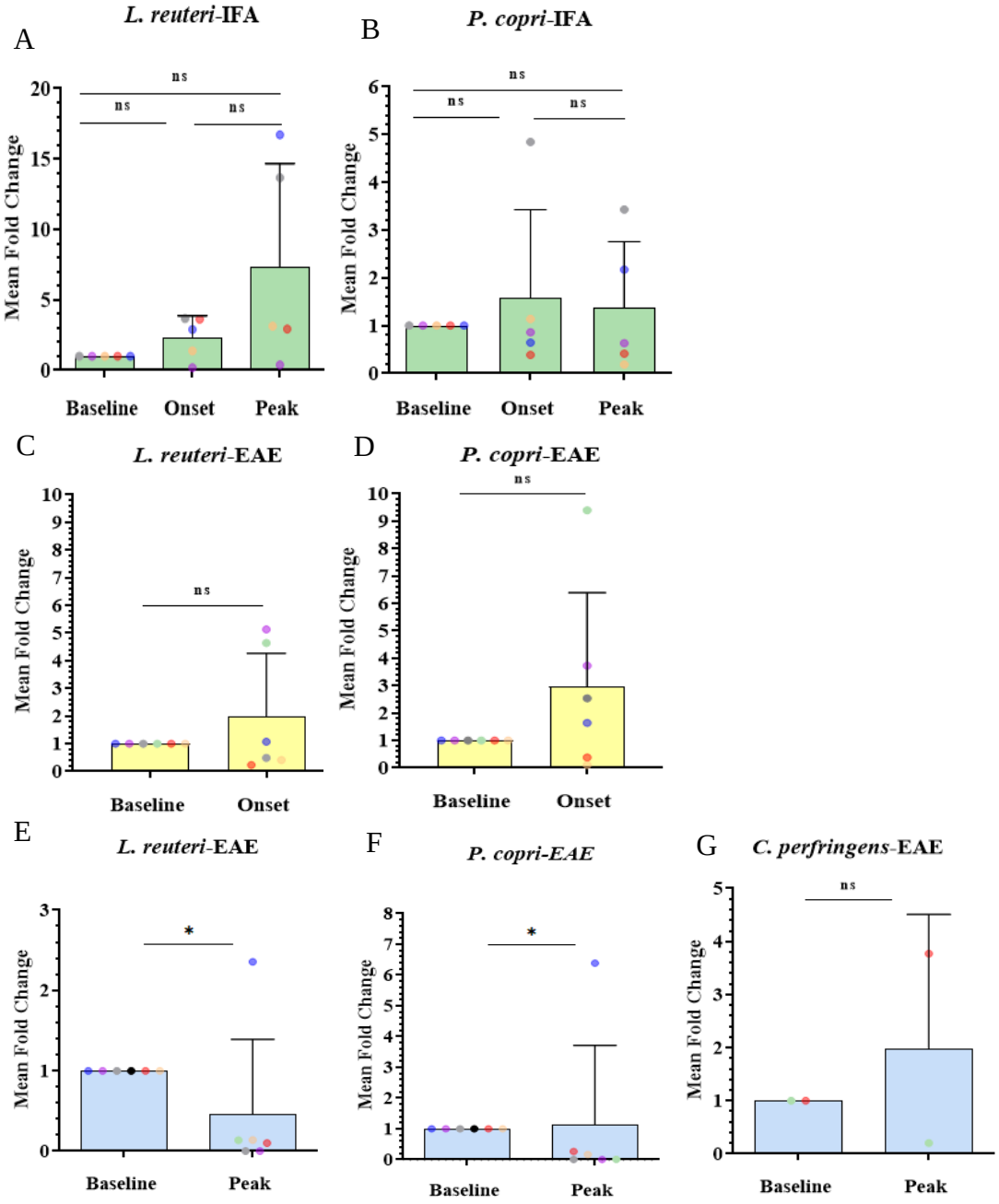

Figure 14: Average fold change of *L. reuteri*, *P. copri*, and *C. perfringens* in control (n=5), diseased-onset (n=6), and diseased- peak (n=6) groups. (A & B): Mean fold change of both *L. reuteri* and *P. copri* in control group at 3 time points. (C & D): Average fold change of *L. reuteri* and *P. copri* in the diseased-onset group at baseline and onset only. (E, F, & G): Mean fold change of the *species L. reuteri*, *P. copri*, and *C. perfringens* in the diseased-peak group at baseline and peak. All results are expressed as mean ± SD. Mann–Whitney U test was performed to determine P values (* $P \leq 0.05$, ns $P > 0.05$). Each colored dot represents fold changes in one mouse throughout the study.

3.7 Correlation between the Detected Species

Table 3 shows Spearman's r correlation computed to spot the light on the relationship between the detected species in our animal model. There was a strong, significant, positive correlation between *L. reuteri* and *P. copri*, with a correlation coefficient equals to 0.77 and P<0.001. Also, spearman's correlation showed that *C. perfringens* has a moderate negative association with *P. copri* (r=-0.40) and a strong negative correlation, but not significant with *L. reuteri* (r=-0.800) indicating that the sample size perhaps not sufficient. Overall, this data represents that whenever the abundancy of *L. reuteri* increases *P. copri* increases as well, whereas *C. perfringens* decreases and vice versa.

Table 3: The association between gut microbes

			L. reuteri	***P. copri***	***C. perfringens***
Spearman's rho	***L. reuteri***	r		0.770**	-0.800
		P-value		<0.001	0.200
	P. copri	r	0.770**		-0.400
		P-value	<0.001		0.600
	C. perfringens	r	-0.800	-0.400	
		P-value	0.200	0.600	

**. Correlation is significant at the 0.01 level (2-tailed).

3.8 Correlation of the Immune Cells with each Bacterial Species

Table 4 illustrates Spearman's r correlation between the intestinal immune cells and the selected bacterial species. Even so, all P values were not significant, Spearman's correlation highlights the association between the variables. There was a weak negative association between *L. reuteri* and both intestinal $CD4^+$ T cells and NK cells (r=0.245 r=-0.218, respectively). Means that the abundance of *L. reuteri* is correlated

with the expansion of both intestinal $CD4^+$ T cells and NK cells. Same results were obtained for the correlation of *P. copri* with $CD4^+$ T cells and NK cells; both are negatively correlated with *P.copri* (r=-0.406 r=-0.14, respectively).

Opposite results were obtained between *C. perfringens* and intestinal $CD4^+$ T cells and NK cells. A strong positive correlation was found between *C. perfringens* and $CD4^+$ T cells (r=0.80) and a weak positive correlation with NK cells (r=0.20). So, the abundancy of *C. perfringens* in the gut is associated with the overall levels of both intestinal $CD4^+$ T and NK cells. $CD8^+$ T cells showed relatively no correlation with any of the detected bacteria.

Table 4: The association between gut immune cells and the gut microbes

			iCD4$^+$	**iCD8$^+$**	**iNK**
Spearman's rho	***L. reuteri***	r	-0.245	0.192	-0.218
		P-value	0.284	0.405	0.342
	P. copri	r	-0.406	0.127	-0.14
		P-value	0.067	0.584	0.953
	C. perfringens	r	0.800	0	0.200
		P-value	0.200	1	0.800

3.9 Paneth Cells

Paneth cells are known for their role in maintaining gut homeostasis. They were studied to investigate whether they are associated with dysbiosis and its correlation with EAE. Paneth cells in the proximal (Duodenum) and distal (Ileum) regions of the small intestine were counted in both control and EAE mice. Also, the raw integrated density (Fluorescence intensity) presented by fold change was obtained using ImageJ software.

Figure 15 demonstrates Paneth cells in the duodenum and ileum stained with H&E and UEA I lectin. Labeled Paneth cells are located at the bottom of the crypts. It seems that Paneth cells are more prominent in the diseased tissue than in the control. Quantification as shown in Figure 16 shows that Paneth cell counts in the duodenum are higher in the diseased mice than in the control ($P>0.0001$). In the ileum, Paneth cells also increased significantly in the diseased mice ($P=0.0108$). Further, the intensity of the fluorescence label reflects the amount of cytoplasmic fucose that binds to the lectin. The labeling intensity was also found to be significantly higher in the duodenum and ileum of the diseased mice ($P>0.0001$) (Figure 17). In addition, correlation analysis was computed to prove that the association between the intensity and the cell count is directly proportional. Although the correlation coefficient factor was 0.241 for ileum and 0.338 for duodenum, it was statistically significant ($P\leq0.05$). Meaning that both Paneth cells and its component increase or decrease together.

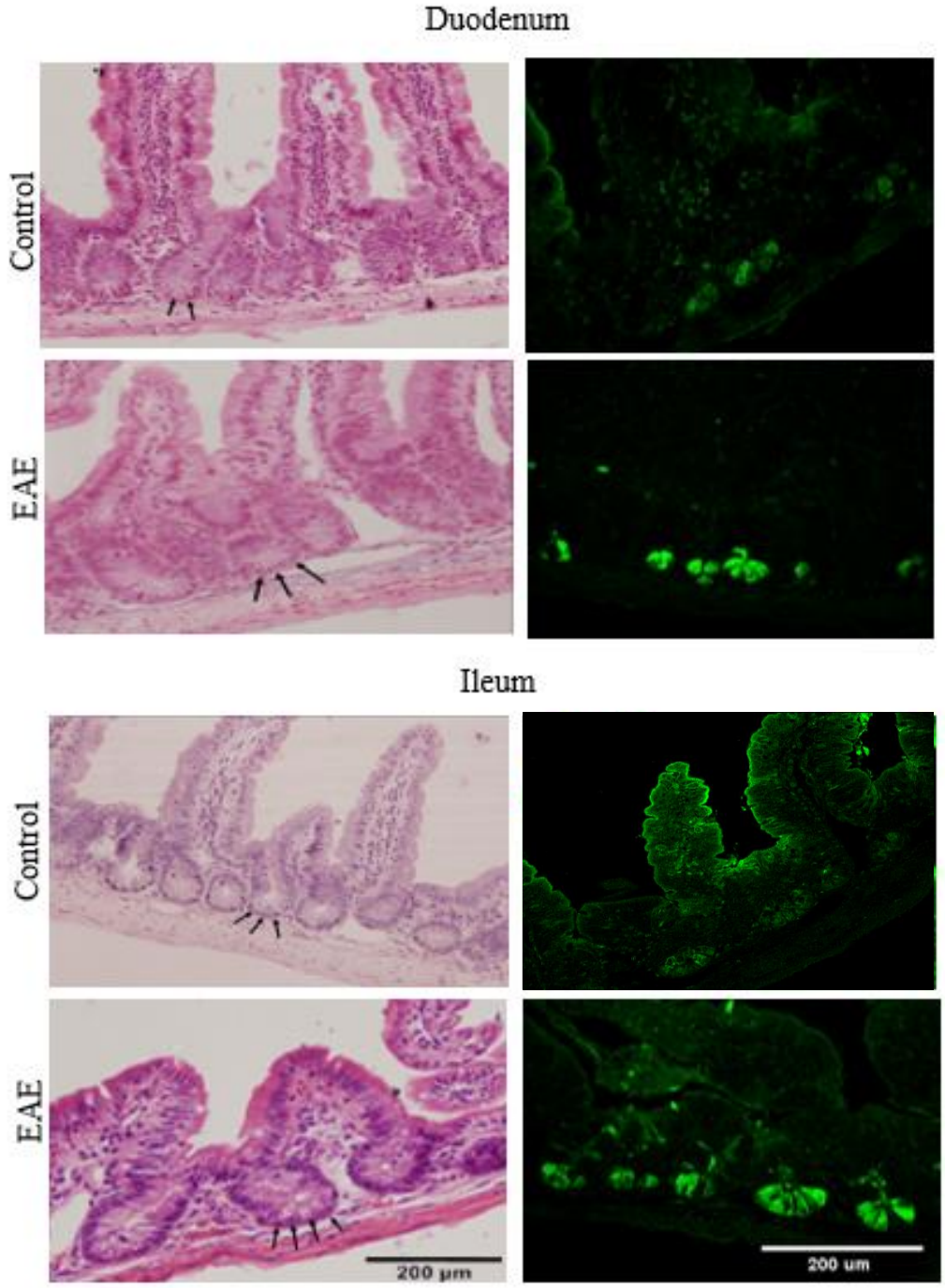

Figure 15: Paneth cells located in the duodenum and ileum of control (n=3) and diseased (n=3) mice stained with lectin (UEA I) (Right) and H & E staining (Left). Bar= 200 µm/ 40x magnification.

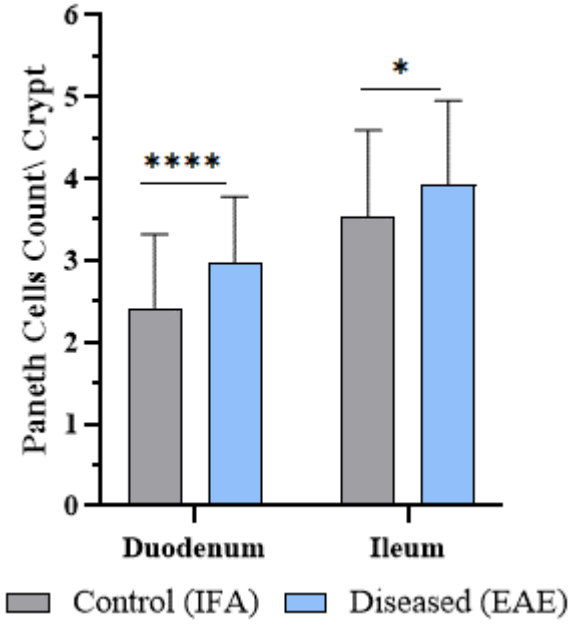

Figure 16: Number of Paneth cells per crypt located in the duodenum and ileum of control and diseased mice (n=3). Results described are from one experiment and expressed as mean ± SD. Mann–Whitney U test was performed to determine P values. (* P≤0.05, ****P≤0.0001).

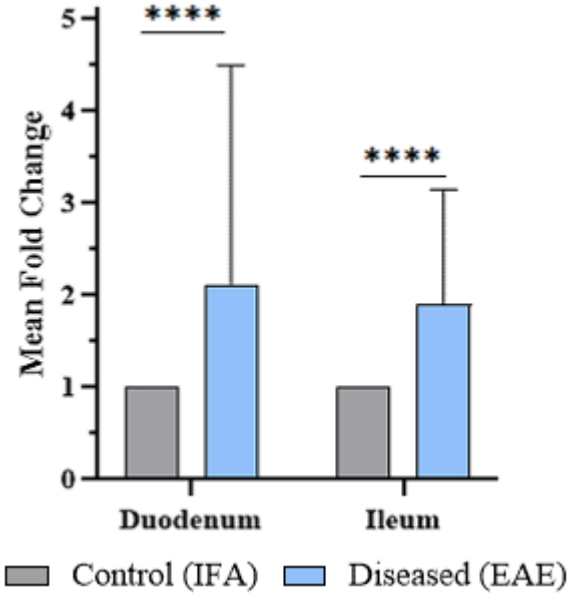

Figure 17: Mean fold change of UEA-I labeling intensity of Paneth cells in duodenum and ileum of control and diseased mice (n=3). Results described are from one experiment and expressed as mean ± SD. Mann–Whitney U test was performed to determine P values (****P≤0.0001).

Chapter 4: Discussion

MS is a highly prevalent autoimmune disease targeting the CNS causing various neurological symptoms leading to a complete paralysis at a certain stage. This disease remains neither curable nor easily detectable at early stages due to the complex factors that may be involved in its initiation and pathogenicity. The prevalence of MS among different regions was investigated, and UAE was classified as a medium-risk country by Kurtzke in 1975; since then, the prevalence of the disease elevated in the region and recorded the highest prevalence among all Asian countries (Etemadifar et al., 2020; Forouhari et al., 2021). Even though the disease etiology is yet to be identified, effective role of activated autoreactive $CD4^+$ and $CD8^+$ T cells has been well established compared to NK cells whose role is still controversial (Dendrou et al., 2015). Since that the main trigger of MS is unknown, many theories were established in the association between MS and environmental or genetic factors. Gut microbiota is strongly believed to be associated with MS where rapid change of the gut microbiota composition was observed in MS patients and same observation was reported in the animal models of the disease (EAE) (Ochoa-Repáraz et al., 2017). Yet, not much work was done to study the interaction between dysbiosis and gut immune cells affecting the outcome of the disease. In the current study, our aim was to investigate and correlate disease severity, percentage of lymphocytes isolated from the small intestine, and changes in the level of selected bacterial species that were previously reported in studies in MS.

Successful disease induction in female C57BL/6 mice was confirmed by noticeable weight loss over the study period (20 days) indicating systemic disease. Weight loss was associated with increase in the clinical score as mice progressed through the

disease as reported in other studies (Burrows et al., 2019; Horstmann et al., 2013; Johanson et al., 2020). Histological analysis confirmed the infiltration of mononuclear cells to the CNS of diseased mice and their aggregation in the white matter at the peak of the disease. Increased level of infiltrating cells was also mirrored by advanced level of demyelination in the white matter estimated with a maximum percentage of 90-100% (Al-Shamsi et al., 2015; Maeda et al., 2019). Furthermore, assessment of frequencies of lymphocytes in the circulation at the different time points showed that $CD4^+$ T cells contributing to the disease pathogenesis was found elevated as the disease progress. Our results are in line with (Saligrama et al., 2019) who found high levels of $CD4^+$ T cells in the blood of immunized mice (Kuchroo et al., 2002; Sonar & Lal, 2017). Our results did not reveal any changes in $CD8^+$ T cells frequencies during the course of the disease which may be in line with other studies suggesting that $CD8^+$ T cells is associated with the pathogenesis of the diseases in MBP induced animal model whereas $CD4^+$ T cells are associated with MOG induced EAE (Huseby et al., 2001). Additionally, it is possible that $CD4^+$ and $CD8^+$ T cells are not engaged in the disease at the same time; it was reported that $CD4^+$ T cells are engaged in the early stages of the disease while $CD8^+$ T cells engaged in late stages which might provide another justification for our findings (Sonobe et al., 2007). Although investigations on the role of NK cells in the pathogenesis in EAE yielded controversial results, most studies lean toward the idea that NK cells exert a regulatory role in the disease (Xu & Tabira, 2011; B. Zhang et al., 1997). Surprisingly, our results showed an increase in the number of peripheral NK cells with a downregulation of the activating receptor NKG2D at the onset of the disease compared to the control which suggest that the activity of the cells was impaired at the onset. In comparison to the changes at the peak, their percentage was lower compared to the onset with no change in their activity status. Depletion

studies may explain the impairment of the NK cells, yet we suggest that NK cells got expanded in response to the antigen at the disease onset, but they at that time point were not expressing NKG2D as it is normally expressed in low levels and increase as they mature.

Furthermore, gut $CD4^+$ and $CD8^+$ T cells did not change throughout the disease as expected though, a previous study proved that during EAE, Th1 and Th17 cells were proliferated while Treg cells were reduced in the Peyer's patches, lamina propria, and mesenteric lymph nodes (Nouri et al., 2014). Most of the studies focusing on the subsets of T cells to define their role while we focused on the total $CD4^+$ T cells so, it might be that some of the T cells subsets were proliferated, but it was not possible to identify the expanding subset since we were looking into the whole population. Yet, Spearman's r we computed showed that there was a positive correlation between $CD4^+$ T cells and NK cells that is suggested to be associated with the severity of the disease supported by our primary observations of circulating lymphocytes. The percentage of $CD8^+$ T cell is believed to be elevated at the site of inflammation (CNS) of MS patients as supported by (Salou et al., 2015). Therefore, it is less likely to be affected among IELs since we are looking to the changes in the composition of the normal flora as they are more engaged in virus eradication and killing tumor cells (Berg & Forman, 2006).

The role of NK cells in maintaining gut homeostasis is known, but investigating gut NK cells profile during the course of EAE was not studied before. In the present study, we found that, frequencies of NK cells in the circulation were inversely proportional to their frequencies in the gut at disease onset and peak. When gut NK cells frequency was low at the onset, it reached its highest frequency in the circulation and vice versa at the peak of the disease. Our findings suggest that NK cells can migrate from the

blood to the tissues. As for the levels and activity of NK cells, mice were sacrificed at the onset retain their total number of NK cells, but the cells expressing the activating receptors were lower than the control. While the mice sacrificed at the peak, a noticeable increase was observed in the number of the total NK cells isolated from the IELs as well as the number of cells expressing the activating (NKG2D) receptor in comparison to the onset. Since the data is limited, and studies on other autoimmune disease such as inflammatory bowel disease showed controversial results raising the question whether NK cells are pathogenic or regulatory as they have both stimulatory and inhibitory receptors, we are suggesting that the down regulation of the NKG2D at the onset might be due to the persistent exposure to its ligand as described previously. Alteration of the number and activation at the peak might be due to the severe changes in the gut composition at this time point (Petit et al., 1985; Yadav et al., 2011). Overall, studies showed that giving probiotics to healthy individuals enhanced the number and activation of NK cells, proving the interaction between NK cells and the gut flora (Aziz & Bonavida, 2016).

Our findings showed that the microbiota composition in control and diseased C57BL/6 mice in the studied species: *L. reuteri, P. copri* and *C. perfringens* was similar to the previous findings. *L. reuteri* was reported to be reduced in MS patients and EAE induced mice compared to healthy controls, and it was used as a probiotic to reduce the severity of symptoms (Chen et al., 2016; Freedman et al., 2018; Gandy et al., 2019; Johanson et al., 2020). *P. copri* was reported to be decreased in MS patients diagnosed with the relapsing remitting form of the disease and their abundance increased during the treatment course, but nothing was reported in EAE induced mice (Shahi et al., 2017). Nevertheless , this specie was found to be associated with the pathogenesis of rheumatoid arthritis, mainly because of its capacity in inducing differentiation of Th17

cells that play a pathological role in MS/EAE (Langrish et al., 2005). As for *C. perfringens, it* is normally known as a pathogenic bacterium. In our EAE model, only 2 mice showed positive results to this specie, one of them was increased during the course of the disease and the other one decreased. A possible explanation is the result of Rumah et al. (2013) who found antibodies specific to epsilon toxin (ETX) produced by C. *perfringens* type B in 10% of their MS patients compared to only 1% of healthy individuals. This toxin thought to be associated with the perturbation of the BBB (Wagley et al., 2019). On the other hand, Rumah et al. (2013) findings showed that *C. perfringens* type A, the common commensal specie, was found in 50% of their healthy individuals compared to 23% only among MS patients. This might explain the variation we got, since we did not define which type of *C. perfringens* our mice had.

In addition, we investigated Paneth cells, one of the defense mechanisms against microbial invasion. The increase in Paneth cells count (Hyperplasia) or their decrease varies among different diseases where it was found to be reduced and impaired during viral infections like HIV, while it increased in IBD (Kelly et al., 2004). Several studies investigated the association between gut microbiota and MS, but this is the first time that association of Paneth cells hyperplasia or metaplasia with MS is being investigated. In our EAE model, we found that at the peak of the disease, mice showed increased number of cells in both duodenum and ileum approximately 10 Paneth cells per 10 crypts and increased lectin positive cells at both regions. Generally, the count of Paneth cells can be altered as a result of dysbiosis, which is the case in our model, it further confirms the dysbiosis even though, we have selected limited number of species to look at. Moreover, immunohistochemical staining using proliferating cell nuclear antigen (PCNA) antibody from (mbl life science, Japan) was performed on the same intestinal tissues and the results indicated that dividing cells were found to be

higher in count in the diseased mice compared to the control (Appendix Figure 1). Similar findings were noted by (Martinez Rodriguez et al., 2012), who reported an association between hyperplasia of Paneth cells and bacterial infection, proposing that some pathogenic bacteria trigger Paneth cells expansion, but not maturation as their total count increased whereas count of granules inside the Paneth cells were reduced, reflecting their immaturity.

Altogether, it was reported that immune cells migrate to the CNS even before the first sign of the disease appears (Sonobe et al., 2007). The same was expected for the gut as suggested by Berer et al. (2014) , but it was not achieved in the gut of our mouse model (Sonobe et al., 2007). In contrary, changes at the onset were minimal, while it was noticeable at the peak of the disease where the *L. ruteri* and *P.copri* reduced accordingly with the increase in the population of NK cells and the expression of their activating receptor (NKG2D) and this was supported by Spearman's rank correlation that showed negative correlation between NK cells and these 2 species. Normally, beneficial bacteria produce ligands to suppress the expansion of Th17 for example and induce Treg cells. In the case of MS\EAE, the abundancy of beneficial bacteria reduced, and pathogenic bacteria expanded and that was somehow confirmed with the hyperplasia of Paneth cells. Besides, Spearman's rank correlation showed a strong positive correlation between clostridium and $CD4^+$ T cells that is mostly pathogenic along with NK cells, but not with *L. ruteri* and *P.copri*.

Chapter 5: Conclusion

This study revealed that the progression of EAE is possibly due to changes of the gut normal flora. Considering all aspects involved in the study, NK cells showed a significant increase by the time the disease was relatively severe, their activation started to be restored, and dysbiosis was clearly shown at that time point. Elevation of NK cells frequency was negatively correlated with *L. reuteri* that was found decreased, in line with other studies, as well as *P.copri* that was reported in animal model for the first time. Paneth cells hyperplasia verified the dysbiosis that was observed with the limited number of studied bacterial species. Furthermore, based on previous studies confirming the interaction between gut microbes and immune cells, we believe that the interactions of gut flora with gut immune cells facilitate the migration of activated autoreactive cells to the CNS, causing damage and severe symptoms. This process is suggested to be associated with a pathogenic role of NK cells, as their number and activation status were altered throughout the disease along with $CD4^+$ T cells that are known for their role in the pathogenesis.

5.1 Limitation and Future Work

Limitations in this study were mainly in the limited number of mice available to conduct the study, which led to the variation in the experimental groups. For the same reason we are not able to look into the count of Paneth cells at different stages. Also, looking at the recovery stage of the disease, as in what is promoting recovery. This is in addition to limited data found on the profile of gut immune cells in MS especially in IELs. This study opens the way to study the subsets of $CD4^+$ T cells; Th1, Th17, T_{reg}, and Th2 and their cytokines; these are the main cells involved in MS that will

help us comprehend the type of immune response achieved in in the gut in relation to variations in the gut flora composition. As for NK cells, our efforts in analyzing their subsets were not successful, but for future work we may identify the subsets and the expression of other receptors on NK cells including NKp46 receptor and lectin-like receptors belongs to Ly49 family. Besides, running a cytotoxic assay would have also provided a better understanding of the role of NK cells. The migration of the gut immune cells to the CNS may be confirmed by immunohistochemistry. For better studying of the gut normal flora and correlating it with all the previous factors, next-generation sequencing is a better option where it can detect a very low quantity of bacteria in the sample, unlike qPCR. For further confirmation on the role of NK cells/gut microbiota interaction, NK cell homing receptor may be blocked followed by studying the bacterial populations and observing the outcome of the disease.

References

Abel, A. M., Yang, C., Thakar, M. S., & Malarkannan, S. (2018). Natural Killer Cells: Development, Maturation, and Clinical Utilization. *Frontiers in Immunology*, *9*, 1869. doi: 10.3389/fimmu.2018.01869

Al-Shamsi, M., Shahin, A., Ibrahim, M. F., Tareq, S., Souid, A.-K., & Mensah-Brown, E. P. (2015). Bioenergetics of the spinal cord in experimental autoimmune encephalitis of rats. *BMC Neuroscience*, *16*(1), 1–13

Ascherio, A., & Munger, K. L. (2007). Environmental risk factors for multiple sclerosis. Part I: The role of infection. *Annals of Neurology*, *61*(4), 288–299.

Azad, M. B., Konya, T., Maughan, H., Guttman, D. S., Field, C. J., Chari, R. S., Sears, M. R., Becker, A. B., Scott, J. A., & Kozyrskyj, A. L. (2013). Gut microbiota of healthy Canadian infants: Profiles by mode of delivery and infant diet at 4 months. *Cmaj*, *185*(5), 385–394

Aziz, N., & Bonavida, B. (2016). Activation of natural killer cells by probiotics. *Onco Therapeutics*, *7*(1–2)

Baecher-Allan, C., Kaskow, B. J., & Weiner, H. L. (2018). Multiple sclerosis: Mechanisms and immunotherapy. *Neuron*, *97*(4), 742–768

Banks, W. A. (2009). Characteristics of compounds that cross the blood-brain barrier. *BMC Neurology*, *9*(1), 1–5

Barry, M., & Bleackley, R. C. (2002). Cytotoxic T lymphocytes: All roads lead to death. *Nature Reviews Immunology*, *2*(6), 401–409

Berer, K., Boziki, M., & Krishnamoorthy, G. (2014). Selective accumulation of pro-inflammatory T cells in the intestine contributes to the resistance to autoimmune demyelinating disease. *PLoS One*, 9(2), e87876. https://doi.org/10.1371/journal.pone.0087876

Berer, K., Mues, M., Koutrolos, M., Rasbi, Z. A., Boziki, M., Johner, C., Wekerle, H., & Krishnamoorthy, G. (2011). Commensal microbiota and myelin autoantigen cooperate to trigger autoimmune demyelination. *Nature*, *479*(7374), 538–541

Berg, R. E., & Forman, J. (2006). The role of CD8 T cells in innate immunity and in antigen non-specific protection. *Current Opinion in Immunology*, *18*(3), 338–343. https://doi.org/10.1016/j.coi.2006.03.010

Bert, A., Gran, B., & Weissert, R. (2011). EAE: Imperfect but useful models of multiple sclerosis. *Trends in Molecular Medicine*, *17*(3), 119–125

Blum, K. S., & Pabst, R. (2007). Lymphocyte numbers and subsets in the human blood: Do they mirror the situation in all organs?. *Immunology Letters*, *108*(1), 45–51

Boussamet, L., Rajoka, M. S. R., & Berthelot, L. (2022). Microbiota, IgA and Multiple Sclerosis. *Microorganisms*, *10*(3), 617. https://doi.org/10.3390/microorganisms10030617

Braniste, V., Al-Asmakh, M., Kowal, C., Anuar, F., Abbaspour, A., Tóth, M., Korecka, A., Bakocevic, N., Ng, L. G., Guan, N. L., Kundu, P., Gulyás, B., Halldin, C., Hultenby, K., Nilsson, H., Hebert, H., Volpe, B. T., Diamond, B., & Pettersson, S. (2014). The gut microbiota influences blood-brain barrier permeability in mice. *Science Translational Medicine*, *6*(263), 263ra158. https://doi.org/10.1126/scitranslmed.3009759

Burrows, D. J., McGown, A., Jain, S. A., De Felice, M., Ramesh, T. M., Sharrack, B., & Majid, A. (2019). Animal models of multiple sclerosis: From rodents to zebrafish. *Multiple Sclerosis Journal*, *25*(3), 306–324

Buscarinu, M. C., Fornasiero, A., Romano, S., Ferraldeschi, M., Mechelli, R., Reniè, R., Morena, E., Romano, C., Pellicciari, G., & Landi, A. C. (2019). The contribution of gut barrier changes to multiple sclerosis pathophysiology. *Frontiers in Immunology*, 1916. https://doi.org/10.3389/fimmu.2019.01916

Caligiuri, M. A. (2008). Human natural killer cells. *Blood, The Journal of the American Society of Hematology*, *112*(3), 461–469

Cantarel, B. L., Waubant, E., Chehoud, C., Kuczynski, J., DeSantis, T. Z., Warrington, J., Venkatesan, A., Fraser, C. M., & Mowry, E. M. (2015). Gut microbiota in multiple sclerosis: Possible influence of immunomodulators. *Journal of Investigative Medicine*, *63*(5), 729–734

Castleman, M. J., Dillon, S. M., Purba, C., Cogswell, A. C., McCarter, M., Barker, E., & Wilson, C. (2020). Enteric bacteria induce IFNγ and Granzyme B from human colonic group 1 innate lymphoid cells. *Gut Microbes*, *12*(1), 1667723. doi: 10.1080/19490976.2019.1667723

Cazorla, S. I., Maldonado-Galdeano, C., Weill, R., De Paula, J., & Perdigón, G. D. V. (2018). Oral Administration of Probiotics Increases Paneth Cells and Intestinal Antimicrobial Activity. *Frontiers in Microbiology*, *9*, 736. https://doi.org/10.3389/fmicb.2018.00736

Chairatana, P., & Nolan, E. M. (2017). Defensins, Lectins, Mucins and Secretory Immunoglobulin A: Microbe-Binding Biomolecules that Contribute to Mucosal Immunity in the Human Gut. *Critical Reviews in Biochemistry and Molecular Biology*, *52*(1), 45–56. https://doi.org/10.1080/10409238.2016.1243654

Chen, J., Chia, N., Kalari, K. R., Yao, J. Z., Novotna, M., Paz Soldan, M. M., Luckey, D. H., Marietta, E. V., Jeraldo, P. R., & Chen, X. (2016). Multiple sclerosis patients have a distinct gut microbiota compared to healthy controls. *Scientific Reports*, *6*(1), 1–10.

Chitnis, T. (2007). The Role of CD4 T Cells in the Pathogenesis of Multiple Sclerosis. *International Review of Neurobiology*, *79*, 43–72. https://doi.org/10.1016/S0074-7742(07)79003-7

Chung, H., Pamp, S. J., Hill, J. A., Surana, N. K., Edelman, S. M., Troy, E. B., Reading, N. C., Villablanca, E. J., Wang, S., & Mora, J. R. (2012). Gut immune maturation depends on colonization with a host-specific microbiota. *Cell*, *149*(7), 1578–1593.

Constantinescu, C. S., & Hilliard, B. A. (2005). Adjuvants in EAE. In *Experimental Models of Multiple Sclerosis.* 21371012. doi: 10.1111/j.1476-5381.2011.01302.x. Springer

Danikowski, K. M., Jayaraman, S., & Prabhakar, B. (2017). Regulatory T cells in multiple sclerosis and myasthenia gravis. *Journal of Neuroinflammation*, *14*(1), 1–16.

Delgado, S., & Sheremata, W. A. (2006). The role of CD4+ T-cells in the development of MS. *Neurological Research*, *28*(3), 245–249. https://doi.org/10.1179/016164106X98107

Dendrou, C. A., Fugger, L., & Friese, M. A. (2015). Immunopathology of multiple sclerosis. *Nature Reviews Immunology*, *15*(9), 545–558.

Dhaiban, S., Al-Ani, M., Elemam, N. M., Al-Aawad, M. H., Al-Rawi, Z., & Maghazachi, A. A. (2021). Role of Peripheral Immune Cells in Multiple Sclerosis and Experimental Autoimmune Encephalomyelitis. *Sci*, *3*(1), 12. https://doi.org/10.3390/sci3010012

Dungan, L. S., McGuinness, N. C., Boon, L., Lynch, M. A., & Mills, K. H. G. (2014). Innate IFN-γ promotes development of experimental autoimmune encephalomyelitis: A role for NK cells and M1 macrophages. *European Journal of Immunology*, *44*(10), 2903–2917. https://doi.org/10.1002/eji.201444612

Durrenberger, P. F., Webb, L. V., Sim, M. J. W., Nicholas, R. S., Altmann, D. M., & Boyton, R. J. (2012). Increased HLA-E expression in white matter lesions in multiple sclerosis. *Immunology*, *137*(4), 317–325. https://doi.org/10.1111/imm.12012

Dyment, D. A., Sadnovich, A. D., & Ebers, G. C. (1997). Genetics of multiple sclerosis. *Human Molecular Genetics*, *6*(10), 1693–1698

Earley, H., Lennon, G., Balfe, Á., Coffey, J. C., Winter, D. C., & O'Connell, P. R. (2019). The abundance of Akkermansia muciniphila and its relationship with sulphated colonic mucins in health and ulcerative colitis. *Scientific Reports*, *9*(1), 1–9

Ebers, G. C. (1992). The geography of MS reflects genetic susceptibility. *Journal of Tropical and Geographical Neurology*, *2*, 66–72

Egervärn, M., Roos, S., & Lindmark, H. (2009). Identification and characterization of antibiotic resistance genes in Lactobacillus reuteri and Lactobacillus plantarum. *Journal of Applied Microbiology*, *107*(5), 1658–1668

Erny, D., Hrabě de Angelis, A. L., Jaitin, D., Wieghofer, P., Staszewski, O., David, E., Keren-Shaul, H., Mahlakoiv, T., Jakobshagen, K., Buch, T., Schwierzeck, V., Utermöhlen, O., Chun, E., Garrett, W. S., McCoy, K. D., Diefenbach, A., Staeheli, P., Stecher, B., Amit, I., & Prinz, M. (2015). Host microbiota constantly control maturation and function of microglia in the CNS. *Nature Neuroscience*, *18*(7), Article 7. https://doi.org/10.1038/nn.4030

Espinoza, J. L., & Minami, M. (2018). Sensing bacterial-induced DNA damaging effects via natural killer group 2 member D immune receptor: From dysbiosis to autoimmunity and carcinogenesis. *Frontiers in Immunology*, *9*, 52. https://doi.org/10.3389/fimmu.2018.00052

Etemadifar, M., Nikanpour, Y., Neshatfar, A., Mansourian, M., & Fitzgerald, S. (2020). Incidence and prevalence of multiple sclerosis in persian gulf area: A systematic review and meta-analysis. *Multiple Sclerosis and Related Disorders*, *40*, 101959. doi: 10.1016/j.msard.2020.101959

Fasano, A. (2011). Zonulin and its regulation of intestinal barrier function: The biological door to inflammation, autoimmunity, and cancer. *Physiological Reviews*. 21248165. doi: 10.1152/physrev.00003.2008

Ferlazzo, G., & Moretta, L. (2014). Dendritic cell editing by natural killer cells. *Critical Reviews in Oncogenesis*, *19*(1–2), 67–75. https://doi.org/10.1615/critrevoncog.2014010827

Fink, L. N., Zeuthen, L. H., Christensen, H. R., Morandi, B., Frøkiær, H., & Ferlazzo, G. (2007). Distinct gut-derived lactic acid bacteria elicit divergent dendritic cell-mediated NK cell responses. *International Immunology*, *19*(12), 1319–1327.

Fischer, M. T., Sharma, R., Lim, J. L., Haider, L., Frischer, J. M., Drexhage, J., Mahad, D., Bradl, M., van Horssen, J., & Lassmann, H. (2012). NADPH oxidase expression in active multiple sclerosis lesions in relation to oxidative tissue damage and mitochondrial injury. *Brain*, *135*(3), 886–899.

Forouhari, A., Taheri, G., Salari, M., Moosazadeh, M., & Etemadifar, M. (2021). Multiple sclerosis epidemiology in Asia and Oceania; A systematic review and meta-analysis. *Multiple Sclerosis and Related Disorders*, *54*, 34247103. doi: 10.1016/j.msard.2021.103119

Freedman, S. N., Shahi, S. K., & Mangalam, A. K. (2018). The "gut feeling": Breaking down the role of gut microbiome in multiple sclerosis. *Neurotherapeutics*, *15*(1), 109–125

Ganal, S. C., Sanos, S. L., Kallfass, C., Oberle, K., Johner, C., Kirschning, C., Lienenklaus, S., Weiss, S., Staeheli, P., & Aichele, P. (2012). Priming of natural killer cells by nonmucosal mononuclear phagocytes requires instructive signals from commensal microbiota. *Immunity*, *37*(1), 171–186

Gandy, K., Zhang, J., Nagarkatti, P., & Nagarkatti, M. (2019). The role of gut microbiota in shaping the relapse-remitting and chronic-progressive forms of multiple sclerosis in mouse models. *Scientific Reports*, *9*(1), 1–17

Geva-Zatorsky, N., Sefik, E., Kua, L., Pasman, L., Tan, T. G., Ortiz-Lopez, A., Yanortsang, T. B., Yang, L., Jupp, R., & Mathis, D. (2017). Mining the human gut microbiota for immunomodulatory organisms. *Cell*, *168*(5), 928–943

Gödel, C., Kunkel, B., Kashani, A., Lassmann, H., Arumugam, M., & Krishnamoorthy, G. (2020). Perturbation of gut microbiota decreases susceptibility but does not modulate ongoing autoimmune neurological disease. *Journal of Neuroinflammation*, *17*(1), 1–6

Goodier, M. R. (2010). Intestinal natural killer cells. In *Natural Killer Cells*. 331–344. Elsevier

Guerra, N., Pestal, K., Juarez, T., Beck, J., Tkach, K., Wang, L., & Raulet, D. H. (2013). A selective role of NKG2D in inflammatory and autoimmune diseases. *Clinical Immunology (Orlando, Fla.)*, *149*(3), 24211717. doi: 10.1016/j.clim.2013.09.003. https://doi.org/10.1016/j.clim.2013.09.003

Gulla, S. V., & Thompson, K. E. (2021). *Killer cell lectin-like receptor subfamily G member 1 (KLRG1) depleting antibodies*. Patent No. 11,180,561. Washington, DC: U.S. Patent and Trademark Office

Haghikia, A., Jörg, S., Duscha, A., Berg, J., Manzel, A., Waschbisch, A., Hammer, A., Lee, D.-H., May, C., Wilck, N., Balogh, A., Ostermann, A. I., Schebb, N. H., Akkad, D. A., Grohme, D. A., Kleinewietfeld, M., Kempa, S., Thöne, J., Demir, S., … Linker, R. A. (2015). Dietary Fatty Acids Directly Impact Central Nervous System Autoimmunity via the Small Intestine. *Immunity, 43*(4), 817–829. https://doi.org/10.1016/j.immuni.2015.09.007

Hasselmann, J. P., Karim, H., Khalaj, A. J., Ghosh, S., & Tiwari-Woodruff, S. K. (2017). Consistent induction of chronic experimental autoimmune encephalomyelitis in C57BL/6 mice for the longitudinal study of pathology and repair. *Journal of Neuroscience Methods, 284*, 71–84.

Hawkes, C. H., & Macgregor, A. J. (2009). Twin studies and the heritability of MS: A conclusion. *Multiple Sclerosis Journal*, *15*(6), 661–667.

Heiss, C. N., & Olofsson, L. E. (2019). The role of the gut microbiota in development, function and disorders of the central nervous system and the enteric nervous system. *Journal of Neuroendocrinology, 31*(5), e12684. doi: 10.1111/jne.12684

Hopkins, M. J., Macfarlane, G. T., Furrie, E., Fite, A., & Macfarlane, S. (2005). Characterisation of intestinal bacteria in infant stools using real-time PCR and northern hybridisation analyses. *FEMS Microbiology Ecology*, *54*(1), 77–85. https://doi.org/10.1016/j.femsec.2005.03.001

Horstmann, L., Schmid, H., Heinen, A. P., Kurschus, F. C., Dick, H. B., & Joachim, S. C. (2013). Inflammatory demyelination induces glia alterations and ganglion cell loss in the retina of an experimental autoimmune encephalomyelitis model. *Journal of Neuroinflammation, 10*(1), 1–12.

Huber, M., Heink, S., Pagenstecher, A., Reinhard, K., Ritter, J., Visekruna, A., Guralnik, A., Bollig, N., Jeltsch, K., & Heinemann, C. (2012). IL-17A secretion by CD8+ T cells supports Th17-mediated autoimmune encephalomyelitis. *The Journal of Clinical Investigation*, *123*(1), 247–260

Huseby, E. S., Liggitt, D., Brabb, T., Schnabel, B., Öhlén, C., & Goverman, J. (2001). A Pathogenic Role for Myelin-Specific Cd8+ T Cells in a Model for Multiple Sclerosis. *Journal of Experimental Medicine*, *194*(5), 669–676. https://doi.org/10.1084/jem.194.5.669

Jandhyala, S. M., Talukdar, R., Subramanyam, C., Vuyyuru, H., Sasikala, M., & Reddy, D. N. (2015). Role of the normal gut microbiota. *World Journal of Gastroenterology: WJG*, *21*(29), 8787–8803

Jian, C., Kanerva, S., Qadri, S., Yki-Järvinen, H., & Salonen, A. (2022). In vitro Effects of Bacterial Exposure on Secretion of Zonulin Family Peptides and Their Detection in Human Tissue Samples. *Frontiers in Microbiology*, *13*, 848128. https://doi.org/10.3389/fmicb.2022

Jiang, W., Chai, N. R., Maric, D., & Bielekova, B. (2011). Unexpected role for granzyme K in CD56bright NK cell-mediated immunoregulation of multiple sclerosis. *The Journal of Immunology*, *187*(2), 781–790

Johanson, D. M., Goertz, J. E., Marin, I. A., Costello, J., Overall, C. C., & Gaultier, A. (2020). Experimental autoimmune encephalomyelitis is associated with changes of the microbiota composition in the gastrointestinal tract. *Scientific Reports*, *10*(1), 1–14

Kelly, P., Feakins, R., Domizio, P., Murphy, J., Bevins, C., Wilson, J., ... & Dhaliwal, W. (2004). Paneth cell granule depletion in the human small intestine under infective and nutritional stress. *Clinical and Experimental Immunology*, *135*(2), 303–309. https://doi.org/10.1111/j.1365-2249.2004.02374.x

Kuchroo, V. K., Anderson, A. C., Waldner, H., & Munder, M. (2002). T cell response in experimental autoimmune encephalomyelitis (EAE): Role of self and cross-reactive antigens shaping, tuning, and regulating the autopathogenic T cell repertoire. *Annual Review of Immunology*, *20*, 101-23

Kurtzke, J. F. (1975). A reassessment of the distribution of multiple sclerosis: Part one. *Acta Neurologica Scandinavica*, *51*(2), 110–136

Langrish, C. L., Chen, Y., Blumenschein, W. M., Mattson, J., Basham, B., Sedgwick, J. D., McClanahan, T., Kastelein, R. A., & Cua, D. J. (2005). IL-23 drives a pathogenic T cell population that induces autoimmune inflammation. *The Journal of Experimental Medicine*, *201*(2), 233–240

Lee, N., Llano, M., Carretero, M., Ishitani, A., Navarro, F., López-Botet, M., & Geraghty, D. E. (1998). HLA-E is a major ligand for the natural killer inhibitory receptor CD94/NKG2A. *Proceedings of the National Academy of Sciences*, *95*(9), 5199–5204. https://doi.org/10.1073/pnas.95.9.5199

Liu, M., Liang, S., & Zhang, C. (2021). NK Cells in Autoimmune Diseases: Protective or Pathogenic? *Frontiers in Immunology*, *12*. 624687. https://doi.org/10.3389/fimmu.2021

Liu, Q., Sanai, N., Jin, W.-N., La Cava, A., Van Kaer, L., & Shi, F.-D. (2016). Neural stem cells sustain natural killer cells that dictate recovery from brain inflammation. *Nature Neuroscience*, *19*(2), 243–252. https://doi.org/10.1038/nn.4211

López, M. C., & Holmes, N. (2005). Phenotypical and functional alterations in the mucosal immune system of CD45 exon 9 KO mice. *International Immunology*, *17*(1), 15–25

Lublin, F. D., Reingold, S. C., Cohen, J. A., Cutter, G. R., Sørensen, P. S., Thompson, A. J., Wolinsky, J. S., Balcer, L. J., Banwell, B., & Barkhof, F. (2014). Defining the clinical course of multiple sclerosis: The 2013 revisions. *Neurology*, *83*(3), 278–286

Luckheeram, R. V., Zhou, R., Verma, A. D., & Xia, B. (2012). CD4+T Cells: Differentiation and Functions. *Clinical and Developmental Immunology*, *2012*, 925135. https://doi.org/10.1155/2012/925135

Lueschow, S. R., & McElroy, S. J. (2020). The Paneth cell: The curator and defender of the immature small intestine. *Frontiers in Immunology*, *11*, 587. https://doi.org/10.3389/fimmu.2020.00587

Lukic, M. L., Saleh, A. M., Mensah-Brown, E., Camasamudram, V., Shahin, A., & Zouali, M. (2003). Strain differences in susceptibility to experimental allergic encephalomyelitis in rats: Molecular regulation at the level of the target tissue. *NATO SCIENCE SERIES SUB SERIES I LIFE AND BEHAVIOURAL SCIENCES*, *354*, 29–43.

Ma, Q., Xing, C., Long, W., Wang, H. Y., Liu, Q., & Wang, R.-F. (2019). Impact of microbiota on central nervous system and neurological diseases: The gut-brain axis. *Journal of Neuroinflammation*, *16*(1), 30823925. https://doi.org/10.1186/s12974-019-1434-3

Madan, J. C., Hoen, A. G., Lundgren, S. N., Farzan, S. F., Cottingham, K. L., Morrison, H. G., Sogin, M. L., Li, H., Moore, J. H., & Karagas, M. R. (2016). Association of cesarean delivery and formula supplementation with the intestinal microbiome of 6-week-old infants. *JAMA Pediatrics*, *170*(3), 212–219.

Maeda, Y., Nakagomi, N., Nakano-Doi, A., Ishikawa, H., Tatsumi, Y., Bando, Y., Yoshikawa, H., Matsuyama, T., Gomi, F., & Nakagomi, T. (2019). Potential of adult endogenous neural stem/progenitor cells in the spinal cord to contribute to remyelination in experimental autoimmune encephalomyelitis. *Cells*, *8*(9), 31484369. doi: 10.3390/cells8091025

Martin, S. M., Mehta, I. K., Yokoyama, W. M., Thomas, M. L., & Lorenz, R. G. (2001). Development of intestinal intraepithelial lymphocytes, NK cells, and NK 1.1+ T cells in CD45-deficient mice. *The Journal of Immunology*, *166*(10), 6066–6073

Martinez Rodriguez, N. R., Eloi, M. D., Huynh, A., Dominguez, T., Lam, A. H. C., Carcamo-Molina, D., Naser, Z., Desharnais, R., Salzman, N. H., & Porter, E. (2012). Expansion of Paneth Cell Population in Response to Enteric Salmonella enterica Serovar Typhimurium Infection. *Infection and Immunity*, *80*(1), 266–275. https://doi.org/10.1128/IAI.05638-11

McMahon, E. J., Bailey, S. L., Castenada, C. V., Waldner, H., & Miller, S. D. (2005). Epitope spreading initiates in the CNS in two mouse models of multiple sclerosis. *Nature Medicine*, *11*(3), 335–339

Meng, Q., Cai, C., Sun, T., Wang, Q., Xie, W., Wang, R., & Cui, J. (2015). Reversible ubiquitination shapes NLRC5 function and modulates NF-κB activation switch. *Journal of Cell Biology*, *211*(5), 1025–1040

Milo, R., & Kahana, E. (2010). Multiple sclerosis: Geoepidemiology, genetics and the environment. *Autoimmunity Reviews*, *9*(5), A387–A394

Miyake, S., Kim, S., Suda, W., Oshima, K., Nakamura, M., Matsuoka, T., Chihara, N., Tomita, A., Sato, W., & Kim, S.-W. (2015). Dysbiosis in the gut microbiota of patients with multiple sclerosis, with a striking depletion of species belonging to clostridia XIVa and IV clusters. *PloS One*, *10*(9), e0137429. doi: 10.1371/journal.pone.0137429

Molfetta, R., Quatrini, L., Santoni, A., & Paolini, R. (2017). Regulation of NKG2D-Dependent NK Cell Functions: The Yin and the Yang of Receptor Endocytosis. *International Journal of Molecular Sciences*, *18*(8), 28767057. https://doi.org/10.3390/ijms18081677

Nagpal, R., Ogata, K., Tsuji, H., Matsuda, K., Takahashi, T., Nomoto, K., Suzuki, Y., Kawashima, K., Nagata, S., & Yamashiro, Y. (2015). Sensitive quantification of Clostridium perfringens in human feces by quantitative real-time PCR targeting alpha-toxin and enterotoxin genes. *BMC Microbiology*, *15*(1), 1–12

Namer, I. J., Steibel, J., Poulet, P., Mauss, Y., Mohr, M., & Chambron, J. (1994). The Role of Mycobacterium tuberculosis in Experimental Allergic Encephalomyelitis. *European Neurology*, *34*(4), 224–227. https://doi.org/10.1159/000117043

Naparstek, Y., Ben-Nun, A., Holoshitz, J., Reshef, T., Frenkel, A., Rosenberg, M., & Cohen, I. R. (1983). T lymphocyte lines producing or vaccinating against autoimmune encephalomyelitis (EAE). Functional activation induces peanut agglutinin receptors and accumulation in the brain and thymus of line cells. *European Journal of Immunology, 13*(5), 418–423

Naves, R., Singh, S. P., Cashman, K. S., Rowse, A. L., Axtell, R. C., Steinman, L., Mountz, J. D., Steele, C., De Sarno, P., & Raman, C. (2013). The interdependent, overlapping, and differential roles of type I and II IFNs in the pathogenesis of experimental autoimmune encephalomyelitis. *Journal of Immunology (Baltimore, Md.: 1950), 191*(6), 2967–2977. https://doi.org/10.4049/jimmunol.1300419

Nouri, M., Bredberg, A., Weström, B., & Lavasani, S. (2014). Intestinal barrier dysfunction develops at the onset of experimental autoimmune encephalomyelitis, and can be induced by adoptive transfer of auto-reactive T cells. *PloS One, 9*(9), e106335. doi: 10.1371/journal.pone.0106335

Ochoa-Repáraz, J., Magori, K., & Kasper, L. H. (2017). The chicken or the egg dilemma: Intestinal dysbiosis in multiple sclerosis. *Annals of Translational Medicine*, *5*(6), 18–18. https://doi.org/10.21037/atm.2017.01.18

Papaparaskevas, J., Mela, V., Houhoula, D. P., Pantazatou, A., Petrikkos, G. L., & Tsakris, A. (2013). Comparative evaluation of conventional and real-time PCR assays for detecting Bacteroides fragilis in clinical samples. *Journal of Clinical Microbiology*, *51*(5), 1593–1595.

Pascal, M., Perez-Gordo, M., Caballero, T., Escribese, M. M., Longo, M., Luengo, O., Manso, L., Matheu, V., Seoane, E., Serrano, M., Labrador, M., & Mayorga, C. (2018). Microbiome and Allergic Diseases. *Frontiers in Immunology*, *9*, 1584. https://doi.org/10.3389/fimmu.2018.01584

Pawate, S., & Sriram, S. (2010). The role of infections in the pathogenesis and course of multiple sclerosis. *Annals of Indian Academy of Neurology, 13*(2), 20814489. https://doi.org/10.4103/0972-2327.64622

Peiris, M., Monteith, G. R., Roberts-Thomson, S. J., & Cabot, P. J. (2007). A model of experimental autoimmune encephalomyelitis (EAE) in C57BL/6 mice for the characterisation of intervention therapies. *Journal of Neuroscience Methods, 163*(2), 245–254

Petit, A., Erst, P. B., Befus, A. D., Clark, D. A., Rosenthal, K. L., Ishizaka, T., & Bienenstock, J. (1985). Murine intestinal intraepithelial lymphocytes. I. Relationship of a novel Thy-1−, Lyt-1−, Lyt-2+, granulated subpopulation to natural killer cells and mast cells. *European Journal of Immunology*, *15*(3), 211–215. https://doi.org/10.1002/eji.1830150302

Pitt, D., Werner, P., & Raine, C. S. (2000). Glutamate excitotoxicity in a model of multiple sclerosis. *Nature Medicine*, *6*(1), 67–70

Poggi, A., Benelli, R., Venè, R., Costa, D., Ferrari, N., Tosetti, F., & Zocchi, M. R. (2019). Human gut-associated natural killer cells in health and disease. *Frontiers in Immunology*, *10*, 31130953. https://doi.org/10.3389/fimmu.2019.00961

Qiu, Z., & Sheridan, B. S. (2018). Isolating Lymphocytes from the Mouse Small Intestinal Immune System. *Journal of Visualized Experiments : JoVE*, *132*, 57281. https://doi.org/10.3791/57281

Rangachari, M., & Kuchroo, V. K. (2013). Using EAE to better understand principles of immune function and autoimmune pathology. *Journal of Autoimmunity*, *45*, 31–39

Rizzello, V., Bonaccorsi, I., Dongarra, M. L., Fink, L. N., & Ferlazzo, G. (2011). Role of natural killer and dendritic cell crosstalk in immunomodulation by commensal bacteria probiotics. *Journal of Biomedicine and Biotechnology*, 21660136. doi: 10.1155/2011/473097

Rumah, K. R., Linden, J., Fischetti, V. A., & Vartanian, T. (2013). Isolation of Clostridium perfringens type B in an individual at first clinical presentation of multiple sclerosis provides clues for environmental triggers of the disease. *PloS One*, *8*(10), e76359. https://doi.org/10.1371/journal.pone.0076359

Ruppova, K. (2017). *Role of eosinophils in experimental autoimmune encephalomyelitis* [PhD Thesis]. Technische Universität Dresden.Germany

Saikali, P., Antel, J. P., Newcombe, J., Chen, Z., Freedman, M., Blain, M., Cayrol, R., Prat, A., Hall, J. A., & Arbour, N. (2007). NKG2D-Mediated Cytotoxicity toward Oligodendrocytes Suggests a Mechanism for Tissue Injury in Multiple Sclerosis. *Journal of Neuroscience*, *27*(5), 1220–1228. https://doi.org/10.1523/JNEUROSCI.4402-06.2007

Saligrama, N., Zhao, F., Sikora, M. J., Serratelli, W. S., Fernandes, R. A., Louis, D. M., Yao, W., Ji, X., Idoyaga, J., Mahajan, V. B., Steinmetz, L. M., Chien, Y.-H., Hauser, S. L., Oksenberg, J. R., Garcia, K. C., & Davis, M. M. (2019). Opposing T cell responses in experimental autoimmune encephalomyelitis. *Nature*, *572*(7770), 7770. https://doi.org/10.1038/s41586-019-1467-x

Salou, M., Nicol, B., Garcia, A., & Laplaud, D.-A. (2015). Involvement of CD8+ T Cells in Multiple Sclerosis. *Frontiers in Immunology*, *6*. 26635816. doi: 10.3389/fimmu.2015.00604

Salzman, N. H., & Bevins, C. L. (2013). Dysbiosis—A consequence of Paneth cell dysfunction. *Seminars in Immunology*, *25*(5), 334–341. https://doi.org/10.1016/j.smim.2013.09.006

Sanmarco, L. M., Wheeler, M. A., Gutiérrez-Vázquez, C., Polonio, C. M., Linnerbauer, M., Pinho-Ribeiro, F. A., Li, Z., Giovannoni, F., Batterman, K. V., & Scalisi, G. (2021). Gut-licensed IFNγ+ NK cells drive LAMP1+ TRAIL+ anti-inflammatory astrocytes. *Nature*, *590*(7846), 473–479.

Satoh-Takayama, N., Vosshenrich, C. A., Lesjean-Pottier, S., Sawa, S., Lochner, M., Rattis, F., Mention, J.-J., Thiam, K., Cerf-Bensussan, N., & Mandelboim, O. (2008). Microbial flora drives interleukin 22 production in intestinal NKp46+ cells that provide innate mucosal immune defense. *Immunity*, *29*(6), 958–970.

Schroeter, C. B., Huntemann, N., Bock, S., Nelke, C., Kremer, D., Pfeffer, K., Meuth, S. G., & Ruck, T. (2021). Crosstalk of Microorganisms and Immune Responses in Autoimmune Neuroinflammation: A Focus on Regulatory T Cells. *Frontiers in Immunology, 12*. 34691057. doi: 10.3389/fimmu.2021.747143

S eno, A., Maruhashi, T., Kaifu, T., Yabe, R., Fujikado, N., Ma, G., ... & Iwakura, Y. (2015). Exacerbation of experimental autoimmune encephalomyelitis in mice deficient for DCIR, an inhibitory C-type lectin receptor. *Experimental Animals*, *64*(2), 109–119. https://doi.org/10.1538/expanim.14-0079

Shahi, S. K., Freedman, S. N., & Mangalam, A. K. (2017). Gut microbiome in multiple sclerosis: The players involved and the roles they play. *Gut Microbes*, *8*(6), 607–615.

Sonar, S. A., & Lal, G. (2017). Differentiation and transmigration of CD4 T cells in neuroinflammation and autoimmunity. *Frontiers in Immunology,* 29238350. doi: 10.3389/fimmu.2017.01695

Sonobe, Y., Jin, S., Wang, J., Kawanokuchi, J., Takeuchi, H., Mizuno, T., & Suzumura, A. (2007). Chronological changes of CD4+ and CD8+ T cell subsets in the experimental autoimmune encephalomyelitis, a mouse model of multiple sclerosis. *The Tohoku Journal of Experimental Medicine*, *213*(4), 329–339

Stanisavljević, S., Dinić, M., Jevtić, B., \DJedović, N., Momčilović, M., \DJokić, J., Golić, N., Mostarica Stojković, M., & Miljković, \DJor\dje. (2018). Gut microbiota confers resistance of albino oxford rats to the induction of experimental autoimmune encephalomyelitis. *Frontiers in Immunology, 9*, 31315227. doi: 10.3390/nu11071613

Sun, C., Xu, J., Huang, Q., Huang, M., Wen, H., Zhang, C., Wang, J., Song, J., Zheng, M., Sun, H., Wei, H., Xiao, W., Sun, R., & Tian, Z. (2016). High NKG2A expression contributes to NK cell exhaustion and predicts a poor prognosis of patients with liver cancer. *Oncoimmunology*, *6*(1), e1264562. https://doi.org/10.1080/2162402X.2016.1264562

Tett, A., Huang, K. D., Asnicar, F., Fehlner-Peach, H., Pasolli, E., Karcher, N., Armanini, F., Manghi, P., Bonham, K., Zolfo, M., De Filippis, F., Magnabosco, C., Bonneau, R., Lusingu, J., Amuasi, J., Reinhard, K., Rattei, T., Boulund, F., Engstrand, L., … Segata, N. (2019). The Prevotella copri Complex Comprises Four Distinct Clades Underrepresented in Westernized Populations. *Cell Host & Microbe*, *26*(5), 666-679.e7. https://doi.org/10.1016/j.chom.2019.08.018

Thompson, K. K., & Tsirka, S. E. (2017). The Diverse Roles of Microglia in the Neurodegenerative Aspects of Central Nervous System (CNS) Autoimmunity. *International Journal of Molecular Sciences*, *18*(3), 504. https://doi.org/10.3390/ijms18030504

Thursby, E., & Juge, N. (2017). Introduction to the human gut microbiota. *Biochemical Journal*, *474*(11), 1823–1836. https://doi.org/10.1042/BCJ20160510

Titus, H. E., Chen, Y., Podojil, J. R., Robinson, A. P., Balabanov, R., Popko, B., & Miller, S. D. (2020). Pre-clinical and clinical implications of "inside-out" vs."outside-in" paradigms in multiple sclerosis etiopathogenesis. *Frontiers in Cellular Neuroscience*, *14*, 599717. doi: 10.3389/fncel.2020.599717

Traugott, U., Reinherz, E. L., & Raine, C. S. (1983). Multiple sclerosis: Distribution of T cells, T cell subsets and Ia-positive macrophages in lesions of different ages. *Journal of Neuroimmunology*, *4*(3), 201–221

Verbrugghe, P., Van Aken, O., Hållenius, F., & Nilsson, A. (2021). Development of a real-time quantitative PCR method for detection and quantification of Prevotella copri. *BMC Microbiology*, *21*(1), 1–10

Wagley, S., Bokori-Brown, M., Morcrette, H., Malaspina, A., D'Arcy, C., Gnanapavan, S., Lewis, N., Popoff, M. R., Raciborska, D., Nicholas, R., Turner, B., & Titball, R. W. (2019). Evidence of Clostridium perfringens epsilon toxin associated with multiple sclerosis. *Multiple Sclerosis (Houndmills, Basingstoke, England)*, *25*(5), 653–660. https://doi.org/10.1177/1352458518767327

Wang, L., Li, Z., Ciric, B., Safavi, F., Zhang, G.-X., & Rostami, A. (2016). Selective depletion of CD11c+ CD11b+ dendritic cells partially abrogates tolerogenic effects of intravenous MOG in murine EAE. *European Journal of Immunology*, *46*(10), 2454–2466

Waubant, E., Lucas, R., Mowry, E., Graves, J., Olsson, T., Alfredsson, L., & Langer-Gould, A. (2019). Environmental and genetic risk factors for MS: An integrated review. *Annals of Clinical and Translational Neurology*, *6*(9), 1905–1922

Wells, J. M., Brummer, R. J., Derrien, M., MacDonald, T. T., Troost, F., Cani, P. D., Theodorou, V., Dekker, J., Méheust, A., & De Vos, W. M. (2017). Homeostasis of the gut barrier and potential biomarkers. *American Journal of Physiology-Gastrointestinal and Liver Physiology*, *312*(3), G171–G193

Winkler-Pickett, R., Young, H. A., Cherry, J. M., Diehl, J., Wine, J., Back, T., Bere, W. E., Mason, A. T., & Ortaldo, J. R. (2008). In vivo regulation of experimental autoimmune encephalomyelitis by NK cells: Alteration of primary adaptive responses. *The Journal of Immunology*, *180*(7), 4495–4506

Xu, W., Fazekas, G., Hara, H., & Tabira, T. (2005). Mechanism of natural killer (NK) cell regulatory role in experimental autoimmune encephalomyelitis. *Journal of Neuroimmunology*, *163*(1–2), 24–30

Xu, W., & Tabira, T. (2011). The role of natural killer (NK) cells in experimental autoimmune encephalomyelitis (EAE) and multiple sclerosis (MS). *Advances in Neuroimmune Biology*, *1*(1), 87–94

Yadav, P. K., Chen, C., & Liu, Z. (2011). Potential role of NK cells in the pathogenesis of inflammatory bowel disease. *Journal of Biomedicine and Biotechnology*, 21687547. doi: 10.1155/2011/348530

Yokoyama, W. M. (1998). Natural killer cell receptors. *Current Opinion in Immunology*, *10*(3), 298–305

Zhang, B., Yamamura, T., Kondo, T., Fujiwara, M., & Tabira, T. (1997). Regulation of experimental autoimmune encephalomyelitis by natural killer (NK) cells. *The Journal of Experimental Medicine*, *186*(10), 1677–1687

Zhang, J., Markovic-Plese, S., Lacet, B., Raus, J., Weiner, H. L., & Hafler, D. A. (1994). Increased frequency of interleukin 2-responsive T cells specific for myelin basic protein and proteolipid protein in peripheral blood and cerebrospinal fluid of patients with multiple sclerosis. *The Journal of Experimental Medicine*, *179*(3), 973–984

Zhang, X., Feng, J., Chen, S., Yang, H., & Dong, Z. (2019). Synergized regulation of NK cell education by NKG2A and specific Ly49 family members. *Nature Communications*, *10*(1), Article 1. https://doi.org/10.1038/s41467-019-13032-5

Appendix

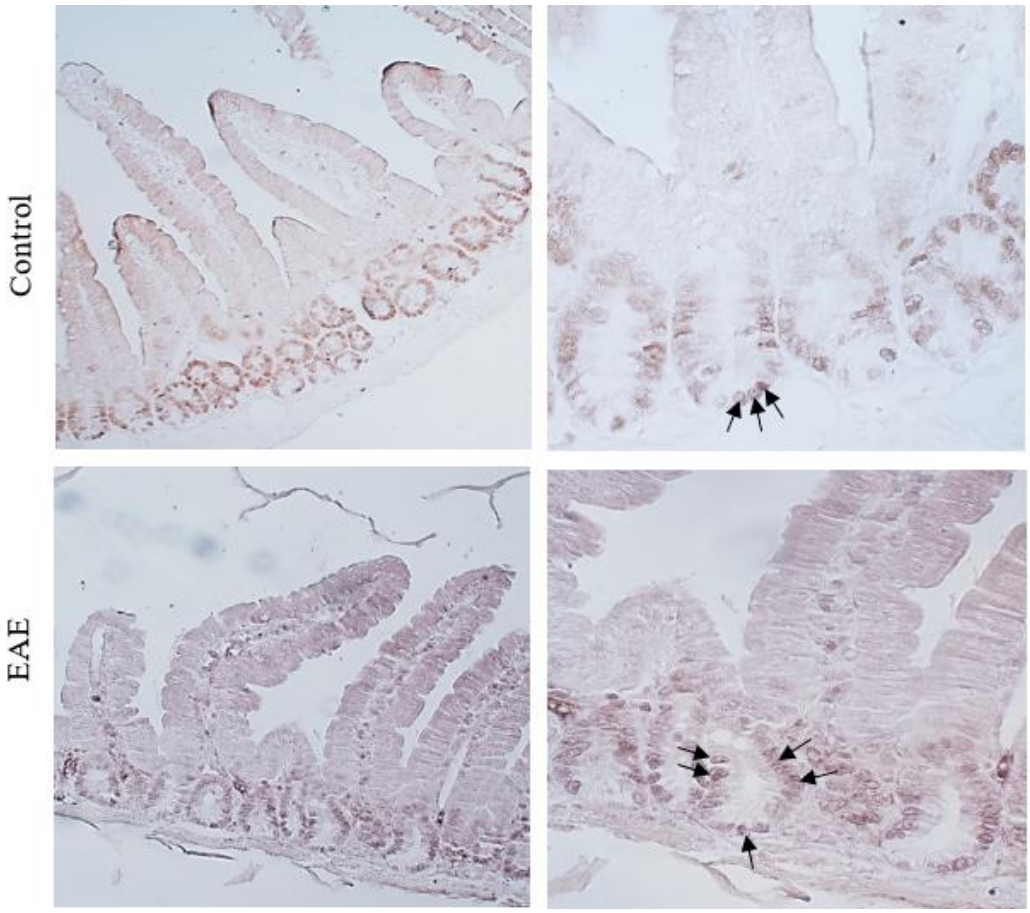

Appendix Figure 1: Dividing cells found in the crypts of Lieberkühn in the intestine of both control and diseased mice stained with PCNA antibody. Magnification is 10x (Left) and 40x (Right).

UAE UNIVERSITY MASTER THESIS NO. 2022:62

This thesis discusses the association between gut alteration and MS/EAE. There is a limited number of studies investigating the link between gut alterations and immune cells in the gut influencing the outcome of the disease since the vast majority of MS patients experience gastrointestinal (GI) problems. Here, we correlate alterations in gut microbiota with disease progression along with changes in lymphocytes counts over different time points during the course of the disease.

Al Anood Ahmed Ali Aldew Al Naqbi received her Master of Medical Sciences from the Department of Medical Microbiology & Immunology, College of Medicine & Health Sciences at UAE University, UAE. She received her BSc in Biology from the College of Science, UAE University, UAE.